Outage Performance Analysis of RSMA-Aided Semi-Grant-Free Transmission Systems

FENGCHENG XIAO[1], XINGWANG LI[2] (Senior Member, IEEE), LIANG YANG[3] (Senior Member, IEEE), HONGWU LIU[1] (Senior Member, IEEE), AND THEODOROS A. TSIFTSIS[4,5] (Senior Member, IEEE)

[1]School of Information Science and Electrical Engineering, Shandong Jiaotong University, Jinan 250357, China

[2]School of Physics and Electronic Information Engineering, Henan Polytechnic University, Jiaozuo 454000, China

[3]College of Computer Science and Electronic Engineering, Hunan University, Changsha 410082, China

[4]School of Intelligent Systems Science and Engineering, Jinan University, Zhuhai 519070, China

[5]Department of Informatics and Telecommunications, University of Thessaly, 35100 Lamia, Greece

CORRESPONDING AUTHOR: H. LIU (e-mail: liuhongwu@sdjtu.edu.cn)

ABSTRACT In this paper, we analyze the outage performance of a rate-splitting multiple access (RSMA)-aided semi-grant-free (SGF) transmission system, in which a grant-based user (GBU) and multiple grant-free users (GFUs) access the base station by sharing the same resource blocks. In the RSMA-aided SGF (RSMA-SGF) transmission system, the GBU and admitted GFU are respectively treated as the primary and secondary users by using the cognitive radio principle. With the aid of RSMA, the admitted GFU's transmit power allocation, target rate allocation, and successive interference cancellation decoding order are jointly optimized to attain the maximum achievable rate for the admitted GFU, without deteriorating the GBU's outage performance compared to orthogonal multiple access. Taking into account the extended non-outage zone achieved by rate-splitting, a closed-form expression is derived for the outage probability of the admitted GFU in the considered RSMA-SGF system. Asymptotic analysis for the admitted GFU's outage probability is also provided. The superior outage performance and full multiuser diversity gain achieved by the RSMA-SGF transmission system are verified by the analytical and simulation results.

INDEX TERMS Grant-free transmissions, multiple access, outage probability, rate-splitting.

I. INTRODUCTION

THE PROLIFERATION of Internet-of-Things (IoT) applications, intelligent robots, and Industry 4.0 networks is resulting in unprecedented needs for massive and spectrally efficient connections. As part of the sixth-generation (6G) evolution roadmap, extremely reliable and low-latency communication (ERLLC), further-enhanced mobile broadband (FeMBB), and ultra-massive machine-type communication (umMTC) have been proposed to enable envisioned heterogeneous 6G applications [1]. For ubiquitous scenarios of umMTC and ERLLC, where traditional grant-based (GB) transmissions are impractical due to the corresponding excessive signaling overhead

and massive computational resource consumption, grant-free (GF) transmissions have been proposed, attracting considerable interests from academia and industry [2], [3], [4]. A main advantage of GF transmissions is that terminals can access the network without engaging in lengthy handshaking, whereas the amount of handshaking signaling can exceed the amount of data sent by terminals in GB transmissions. Although GF transmissions are the promising solutions for massive connectivity, GB transmissions cannot be overlooked due to the stringent quality of service (QoS) requirements of existing grant-based GB users (GBUs). For this reason, semi-grant-free (SGF) transmissions have been proposed to accommodate the coexistence of GB and GF

transmissions, which results in higher spectral efficiency than admitting only GBUs or GF users (GFUs) [5]. To opportunistically admit GFUs to resource blocks occupied by GBUs, non-orthogonal multiple access (NOMA)-aided SGF (NOMA-SGF) transmissions have been proposed, which eliminates complex handshaking processes for admitting GFUs [5], [6]. By using NOMA, user collisions caused by the GFUs' contention can be resolved by spectrum sharing with the aid of successive interference cancellation (SIC).

To avoid system performance degradation of a GBU in the NOMA-SGF transmission system, the GFU's contention must be managed appropriately taking into account the GBU's QoS requirements. Specifically, outage performance experienced by the GBU should be comparable to that of its orthogonal multiple access (OMA) counterpart [5], [6]. In [5], a distributed contention protocol was proposed to guarantee that a fixed number of GFUs are admitted. It was seen that this open-loop protocol suffered from user collisions at a rate similar to that seen in pure GF transmissions. In [6], the received GBU's signal power at the base station (BS) was used to determine an interference threshold, which was then broadcast to GFUs to facilitate distributed contentions. Considering that existing power-domain NOMA schemes rely on superposition coding and transmit power allocation, advanced SIC can be used to maintain a high transmission reliability while preventing the GBU from unnecessary awareness of the GFUs' contention [6], [7], [8]. In [9], a hybrid SIC was proposed to decode the desired signals based on their relative power levels, i.e., the admitted GFU's signal can be decoded at the first or second stage of SIC to attain the allowed maximum achievable rate, which can be used in conjunction with transmit power allocation to further improve the reliability of the NOMA-SGF transmission system [10].

When viewed in the context of underlay cognitive radio (CR), the paired NOMA users can be regarded as a primary user (PU) and a secondary user (SU), respectively [11], which signifies that GB and GF transmissions in NOMA-SGF systems can be treated as primary and secondary transmissions, respectively. Since CR-inspired NOMA (CR-NOMA) with SIC can achieve only a subset on the capacity region boundary of uplink multiple access channels (MACs), the outage performance of SU in this setting can result in decreased user fairness [12]. To avoid deterioration in the PU's outage performance, both PU and SU can be allowed to access the same BS simultaneously in CR-NOMA, and a new hybrid SIC was proposed to improve the achievable rate of the SU in such a system [13]. To achieve arbitrary points on the capacity region boundary of uplink MACs, rate-splitting multiple access (RSMA) proposed in [14] can also be implemented in a CR-inspired way, which can extend the non-outage zone for CR-NOMA [12]. In [15], the authors proposed a CR-inspired RSMA (CR-RSMA) scheme to improve the SU's outage performance by admitting both PU and SU simultaneously to access the same BS. Nevertheless, both PU and SU in the underlay CR-NOMA and CR-RSMA

systems worked in a GB manner [13], [15], whereas a GFU needed to share the same time-frequency resource blocks with a GBU in the SGF transmissions through a shortened hand-shaking signaling. Moreover, the admission contention from multiple GFUs was not taken into account in CR-RSMA and the effects of the GFUs' contention on the RSMA-aided SGF (RSMA-SGF) transmission systems are still unknown.

A. RELATED WORK

1) RSMA: RSMA has received significant attention recently due to its capability to improve the spectral/energy efficiencies, robustness, reliability, and latency of downlink and uplink multi-user transmissions [16], [17]. In downlink RSMA, the users' messages are split into common and private streams using available channel state information at the transmitter (CSIT) [18]. By treating inter-user interference flexibly, i.e., interference can be partially decoded and partially treated as noise, downlink RSMA not only bridges space division multiple access (SDMA) and NOMA, but also achieves superior system performance, so that it is regarded as a promising enabling technology for 6G new radio (NR) [19], [20], [21], [22] (see also [16] and references therein).

However, RSMA and the corresponding applications for uplink MACs are still in their infancy. By using the rate-splitting technique, the message of each user is split into multiple sub-messages to enable non-orthogonal uplink RSMA, which provides flexible interference management, better user-fairness, and massive connectivity as compared to conventional uplink OMA and NOMA [12], [23], [24]. Being essentially different from downlink RSMA, which decodes common and private streams partially at a receiver to balance the decoding performance and complexity, the split data streams from all the users are fully decoded at the BS using SIC in uplink RSMA [23], [24], [25], [26]. In [23], the sum-rate maximization problem was investigated for uplink RSMA in which the proportional rate constraints among users were considered. To enhance the outage performance of uplink NOMA, several rate-splitting schemes were proposed in [24], [25], [26]. For single-input multiple-output (SIMO) NOMA, uplink rate-splitting was investigated to guarantee max-min user fairness in [24]. Nevertheless, an exhaustive search was needed to find the optimal SIC decoding order and optimal power allocation for uplink RSMA [23], [24]. Using the CR principle, adaptive power allocation and rate-splitting were proposed to improve the outage performance and user fairness for uplink NOMA in [12].

Recently, uplink RSMA has been applied to realize physical layer network slicing for ultra-reliable and low-latency (URLLC) and enhanced mobile broadband communications (eMMB) [27]. Also, RSMA has been used to support URLLC and eMMB in 6G NR downlink transmissions [28]. In [29], the outage performance of uplink RSMA was investigated taking into account all possible SIC decoding

orders. In [30], cooperative RSMA was proposed to realize uplink user cooperation. In [31] and [32], rate-splitting schemes were designed for uplink aerial networks and satellite communications, respectively. Rate-splitting applications for cell-free machine-type communications and device-to-device fog radio access networks were investigated in [33] and [34], respectively.

2) NOMA-SGF Transmissions: To control the number of admitted GFUs for the NOMA-SGF transmission system, two contention mechanisms, namely open-loop contention and distributed contention protocols, have been proposed in [5], in which an interference temperature alike channel gain threshold was broadcast to aid the GFUs' contention. Furthermore, a dynamic interference threshold proportional to the received GBU's signal power was proposed in [7] to determine the admitted GFUs, which results in reduced GFUs' interference compared to the open-loop contention. The authors in [6] and [9] proposed CR-NOMA with hybrid SIC decoding order to enhance transmission reliability of the admitted GFU, meanwhile ensuring that the GBU experiences the same outage performance as in OMA. An ergodic rate analysis was provided for NOMA-aided SGF (NOMA-SGF) transmissions in [35]. To efficiently leverage the capability of CR-NOMA to achieve the capacity region of uplink MACs, adaptive power allocation with hybrid and fixed SIC decoding orders were proposed in [8] and [10]. Further, adaptive power allocation was proposed in [36] for the NOMA-SGF transmission system to improve the outage performance and sum rate. In [37], a downlink collided-preamble feedback was applied to facilitate massive multiple-input multiple-output assisted SGF random access. For tactile IoT networks that use NOMA-SGF transmissions, joint power allocation and sub-channel assignment were investigated in [38]. In [39], a user barring scheme was proposed to increase the average arrival rate for the NOMA-SGF transmission system taking into account multiple transmit power levels. In [40] and [41], multi-agent deep reinforcement learning (MADRL) was applied to optimize the transmit power for NOMA-SGF and NOMA-aided GF (NOMA-GF) transmissions. Moreover, MADRL was used to optimize transmit power allocation, sub-channel assignment and reflection beamforming for an intelligent reflecting surface (IRS) aided NOMA-SGF system [42].

B. MOTIVATION AND CONTRIBUTIONS

Although the NOMA-SGF transmissions can accommodate the coexistence of GB and GF transmissions, these systems achieve only a subset of the uplink MAC capacity region as noted above. In contrast, the full capacity region of uplink MACs can be achieved by using RSMA [14]. However, to maximize the sum-rate and ensure user fairness, exhaustive search was used to determine the optimal SIC decoding order and optimal power allocation for uplink RSMA, which is computationally prohibitive [23], [24]. For delay-limited transmissions, the authors in [12] proposed a

CR-inspired transmit power allocation to aid rate-splitting, in which target rates of the SU's data streams were chosen heuristically.

On the other hand, the recently proposed CR-RSMA can improve the SU's outage performance [15] and reduce the task-offloading latency for mobile edge computing [43] by optimizing the transmit power and target rate allocations. Motivated by the capacity region achieved by SGF transmissions, we apply the CR-RSMA that adopts RSMA and CR principles to assist SGF transmissions, with the aim of improving the system performance under the uplink RSMA framework. In the considered RSMA-SGF transmission system, rate-splitting is conducted at the admitted GFU, while the optimal transmit power and target rate allocations at the admitted GFU and SIC decoding order at the BS are jointly optimized using the CR principle, which improves the admitted GFU's outage performance significantly.

The main contributions of this paper are summarized as follows:

- For the RSMA-SGF system, we show that the non-outage zone is extended significantly compared to the NOMA-SGF scheme by exploiting the full capacity region. Due to the extended non-outage zone, additional target rate pairs containing the higher target rates for the admitted GFU are supported by the RSMA-SGF scheme. Therefore, the outage performance of the admitted GFU is significantly improved when RSMA-SGF scheme is applied.
- We derive exact expressions for the outage probability of the admitted GFU and its approximation in the high signal-to-noise ratio (SNR) region. These analytical results reveal that the full multiuser diversity gain is achieved by the RSMA-SGF transmission system. Moreover, benefiting from the obtained maximum achievable rate for the admitted GFU, the multiuser diversity can be achieved in a wider target rate regions than that of the NOMA-SGF transmission system.
- Various computer simulation results are presented to verify the accuracy of the derived analytical results and corresponding high SNR approximations. The superior outage performance of the admitted GFU achieved by the RSMA-SGF scheme is verified by these simulation results. The impacts of the target rate and number of GFUs on the outage performance of the admitted GFU are revealed.

The remainder of this paper is organized as follows: Section II presents the system model and the RSMA-SGF scheme, respectively; In Section III, the outage performance of the admitted GFU achieved by the RSMA-SGF transmission system is analyzed and the high SNR approximation for the outage probability is derived; In Section IV, simulation results are presented for corroborating the superior outage performance of the RSMA-SGF transmission system, and Section V summarizes this work.

II. SYSTEM MODEL AND CR-RSMA TRANSMISSIONS
A. SYSTEM MODEL
We assume that the considered system consists of multiple GBUs and multiple GFUs. To prevent GF transmissions from generating too much interference to GBUs, all the GFUs and GBUs are divided into multiple groups, each of which contains K GFUs and one GBU. In each group, we assume that only one out of K GFUs is paired with the GBU for simultaneous uplink transmissions, whereas multiple GFUs from different groups can be simultaneously admitted through wireless resource allocation among the groups.

Without loss of generality, we consider SGF transmissions within a single group, in which the GBU and the kth GFU are denoted by U_0 and $U_k \in \{U_1, U_2, \ldots, U_K\}$, respectively. The channel coefficients from U_0 and U_k to the BS are denoted by h_0 and h_k ($k = 1, 2, \ldots, K$), respectively, which are modeled as independent and identically distributed (i.i.d.) circular symmetric complex Gaussian random variables with zero mean and unit variance. We assume that the channels follow a quasi-static fading, i.e., the channel coefficients remain constant during a single transmission block and can vary from one transmission block to another independently. Moreover, the channel gains can be ordered as

$$|h_1|^2 \leq |h_2|^2 \leq \cdots \leq |h_K|^2, \tag{1}$$

where the subscripts denote the ordered indices. It should be noted that the above ordering information is unavailable to the K GFUs and the BS. In the considered system, we assume that the K GFUs have the knowledge of their own channel state information (CSI) and the admitted GFU's CSI is not required to be known at the BS prior to the SGF transmissions. In addition, the BS has acquired the information of the GBU's CSI and transmit power. To compare the system performance of the RSMA-SGF scheme with the benchmarks, we also assume perfect SIC at the BS receiver as those in [6], [13].

Without loss of generality, we assume that the ℓth GFU U_ℓ is admitted to transmit ($1 \leq \ell \leq K$). For each block of transmissions, U_ℓ can split its message signal $\bar{x}_\ell$ into two parts $\bar{x}_{\ell,1}$ and $\bar{x}_{\ell,2}$. Corresponding to the message signals $\bar{x}_\ell$, $\bar{x}_{\ell,1}$, and $\bar{x}_{\ell,2}$, the generated transmit signals at U_ℓ are denoted by x_ℓ, $x_{\ell,1}$, and $x_{\ell,2}$, respectively. In each transmission block, U_0 and U_ℓ simultaneously transmit their signals to the BS. Then, the received signal at the BS can be written as:

$$y = \sqrt{P_0}h_0 x_0 + \sqrt{\alpha P_s}h_\ell x_{\ell,1} + \sqrt{(1-\alpha)P_s}h_\ell x_{\ell,2} + w, \tag{2}$$

where P_0 and P_s denote the transmit power of U_0 and U_ℓ, respectively, x_0 is the transmit signal of U_0, α is the transmit power allocation factor at U_ℓ satisfying $0 \leq \alpha \leq 1$, and w is additive white Gaussian noise (AWGN) at the BS with zero mean and unit variance. We assume that each transmit signal $\tilde{x} \in \{x_0, x_\ell, x_{\ell,1}, x_{\ell,2}\}$ is coded by an independent Gaussian code book and satisfies $\mathbb{E}\{|\tilde{x}|^2\} = 1$, where $\mathbb{E}\{\cdot\}$ is the expectation operator.

At the BS, the decoding order $x_{\ell,1} \rightarrow x_0 \rightarrow x_{\ell,2}$ is adopted in SIC to recover the signal $x_{\ell,1}$, x_0, and $x_{\ell,2}$, sequentially. According to [15], the SIC decoding order $x_{\ell,1} \rightarrow x_0 \rightarrow x_{\ell,2}$ ensures that U_ℓ obtains the allowed maximum achievable rate. Also, the full capacity region boundary of MACs can be achieved by applying the SIC decoding order $x_{\ell,1} \rightarrow x_0 \rightarrow x_{\ell,2}$ [14]. Then, the received signal-to-interference-plus-noise ratio (SINR) (or signal-to-noise ratio (SNR)) for decoding $x_{\ell,1}$, x_0, and $x_{\ell,2}$ can be expressed as follows:

$$\gamma_{\ell,1} = \frac{\alpha P_s |h_\ell|^2}{P_0|h_0|^2 + (1-\alpha)P_s|h_\ell|^2 + 1}, \tag{3}$$

$$\gamma_0 = \frac{P_0|h_0|^2}{(1-\alpha)P_s|h_\ell|^2 + 1}, \tag{4}$$

and

$$\gamma_{\ell,2} = (1-\alpha)P_s|h_\ell|^2. \tag{5}$$

For the admitted U_0 and U_ℓ, the achievable rates are given by $R_0 = \log_2(1+\gamma_0)$ and $R_\ell = R_{\ell,1} + R_{\ell,2}$, respectively, with $R_{\ell,1} = \log_2(1+\gamma_{\ell,1})$ and $R_{\ell,2} = \log_2(1+\gamma_{\ell,2})$ representing the achievable rates to transmit $x_{\ell,1}$ and $x_{\ell,2}$, respectively.

Remark 1: By simply interchanging $x_{\ell,1}$ and $x_{\ell,2}$, all possible SIC decoding orders at the BS can be categorized into three types as $x_{\ell,1} \rightarrow x_{\ell,2} \rightarrow x_0$, $x_0 \rightarrow x_{\ell,1} \rightarrow x_{\ell,2}$, and $x_{\ell,1} \rightarrow x_0 \rightarrow x_{\ell,2}$. Using the logarithmic product law, we can readily prove that applying $x_{\ell,1} \rightarrow x_{\ell,2} \rightarrow x_0$ is equal to applying $x_\ell \rightarrow x_0$ in the sense of attaining the achievable rates R_ℓ and R_0. In such a case, rate-splitting is unnecessary, so does the decoding order $x_0 \rightarrow x_{\ell,1} \rightarrow x_{\ell,2}$. As it will be seen in the next subsection, NOMA with the SIC decoding orders $x_\ell \rightarrow x_0$ and $x_0 \rightarrow x_\ell$ cannot approach the full capacity region boundary of MACs. Thus, the decoding order $x_{\ell,1} \rightarrow x_0 \rightarrow x_{\ell,2}$ is used in the RSMA-SGF transmission system with respect to its capability to achieve the full capacity region boundary.

B. RSMA-SGF TRANSMISSIONS
For the considered the RSMA-SGF transmission system, to guarantee that the GBU U_0 achieves the same outage performance as in OMA, a CR analogous interference threshold is broadcast to the K GFUs to aid user contention. Let $\hat{R}_0$, $\hat{R}_s$, $\hat{R}_{s,1}$, and $\hat{R}_{s,2}$ denote the target rates to transmit x_0, x_ℓ, $x_{\ell,1}$, and $x_{\ell,2}$, respectively. In addition, we define $\hat{R}_s = \hat{R}_{s,1} + \hat{R}_{s,2}$, $\hat{R}_{s,1} = \beta\hat{R}_s$, and $\hat{R}_{s,2} = (1-\beta)\hat{R}_s$, where $0 \leq \beta \leq 1$ is the target rate allocation factor. With respect to the SIC decoding order $x_{\ell,1} \rightarrow x_0 \rightarrow x_{\ell,2}$, the signal x_0 can be decoded correctly only when the following constraints are satisfied, i.e.,

$$R_{\ell,1} \geq \hat{R}_{s,1} \quad \text{and} \quad R_0 \geq \hat{R}_0. \tag{6}$$

Under the constraints in (6), the GBU achieves the same outage performance as in OMA when $\Pr(R_{\ell,1} \geq \hat{R}_{s,1}) = 1$ and

$$\Pr\left(R_0 \geq \hat{R}_0\right) = \Pr\left(\log_2\left(1 + P_0|h_0|^2\right) \geq \hat{R}_0\right). \tag{7}$$
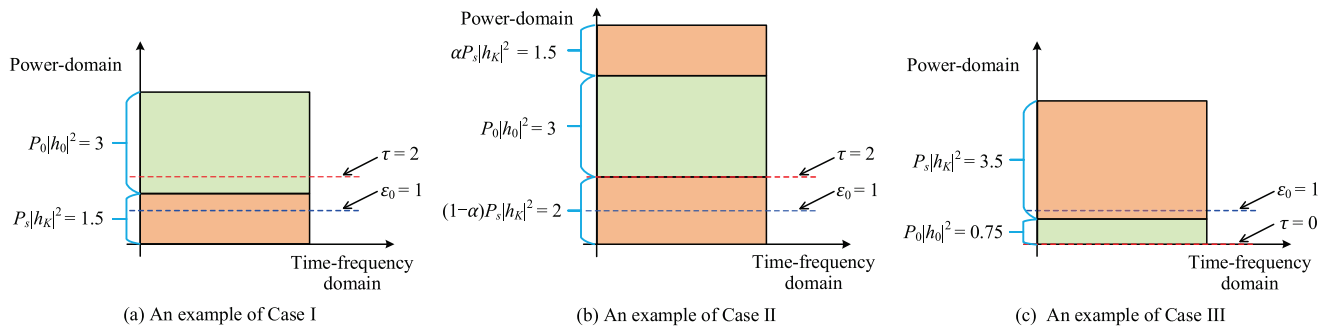
FIGURE 1. An illustration of the received power levels of the RSMA-SGF scheme ($\hat{R}_0 = 1$, $\varepsilon_0 = 1$, and τ is given by (9)).

By substituting (4) into (7), the equality in (7) holds under the condition of

$$(1 - \alpha)P_s|h_\ell|^2 \leq \hat{\tau}, \qquad (8)$$

where $\hat{\tau} = \frac{P_0|h_0|^2}{\varepsilon_0} - 1$ with $\varepsilon_0 = 2^{\hat{R}_0} - 1$. The equation (8) indicates that the interference power caused by the transmission of $\sqrt{(1 - \alpha)P_s}h_\ell x_{\ell,2}$ cannot surpass $\hat{\tau}$ to ensure the correct decoding of x_0 at the second stage of SIC. By assuming that $\Pr(R_{\ell,1} \geq \hat{R}_{s,1}) = 1$ is guaranteed in the RSMA-SGF transmission system, as it will be explained later in this subsection, the interference threshold to be broadcasted by the BS is determined as [6]:

$$\tau = \max\{0, \hat{\tau}\}. \qquad (9)$$

The admission procedure of the RSMA-SGF scheme is presented as follows:

- The BS broadcasts the pilot signals to assist the users to estimate CSI.
- U_0 feeds back its CSI and P_0 to the BS.
- The BS calculates τ according to (9) and broadcasts it to the K GFUs.
- Each GFU calculates the achievable rate using its own CSI and the corresponding optimal α^* and β^*, which will be provided in the later part of this subsection.
- Through the distributed contention, the GFU that obtains the maximum achievable rate is admitted by the BS.

With respect to the capability of uplink RSMA to achieve the full capacity region boundary of MACs, the design goal of the RSMA-SGF scheme is to maximize the achievable rate for the admitted GFU meanwhile guaranteeing that the GBU achieves the same outage performance as in OMA by jointly optimizing the transmit power allocation and target rate allocation. The optimization problem can be formulated as:

$$(P1) : \max_{\alpha, \beta} \ R_\ell$$
$$\text{s.t.} \ \ C1 : \tau \geq 0,$$
$$C2 : 0 \leq \alpha \leq 1,$$
$$C3 : 0 \leq \beta \leq 1. \qquad (10)$$

In (10), C1 is the QoS constraint of U_0, C2 is the constraint of the transmit power allocation, and C3 is the constraint

of the target rate allocation. Considering all the possible QoS realizations of U_0 and all the possible CSI realizations, the received power levels of $P_0|h_0|^2$ and $P_s|h_K|^2$ can be classified into three cases, namely, Case I: $0 < P_s|h_K|^2 \leq \tau$, Case II: $0 < \tau < P_s|h_1|^2$ or $P_s|h_k|^2 < \tau < P_s|h_{k+1}|^2$ with $k = 1, 2, \ldots, K - 1$, and Case III: $\tau = 0$. As an illustration, three examples of the received power levels corresponding to Cases I, II, and III are respectively depicted in Fig. 1. In the following, the optimal α^* and β^* of the RSMA-SGF scheme are jointly designed for Cases I, II, and III, respectively.

Case I: $0 < P_s|h_K|^2 \leq \tau$. In this case, the maximum interference level caused by admitting an arbitrary GFU is not greater than the interference threshold τ. When U_ℓ is admitted, the maximum achievable rate is given by $R_\ell = R_{\ell,2} = \log_2(1 + \gamma_{\ell,2})$ considering that $x_{\ell,2}$ is interference-freely decoded at the last stage of SIC. In other words, U_ℓ will allocate all of P_s to transmit x_ℓ by setting $x_{\ell,2} = x_\ell$. Consequently, U_K, which has the greatest channel gain among all the GFUs, is admitted to attain the maximum achievable rate $R_K = R_{K,2} = \log_2(1 + \gamma_{K,2})$. In this case, the optimal transmit power and target rate allocation factors are respectively given by

$$\alpha^* = 0 \ \text{and} \ \beta^* = 0, \qquad (11)$$

where $(\cdot)^*$ denotes the optimal solution for the corresponding parameter.

Since only $x_{K,2}$ ($x_{K,2} = x_K$) is transmitted, the SIC decoding order $x_{K,1} \rightarrow x_0 \rightarrow x_{K,2}$ degenerates to $x_0 \rightarrow x_K$. Consequently, the achievable rate of the admitted GFU can be expressed as

$$R_K^{(I)} = \log_2\left(1 + P_s|h_K|^2\right). \qquad (12)$$

Case II: $0 < \tau < P_s|h_1|^2$ or $P_s|h_k|^2 < \tau < P_s|h_{k+1}|^2$ *with* $k = 1, 2, \ldots, K - 1$. In this case, it can be seen that $\hat{\tau} > 0$. Then, a GFU U_ℓ whose channel gain is larger than $\hat{\tau}$ will be admitted, where $k + 1 \leq \ell \leq K$. Due to $\hat{\tau} > 0$, the GBU's signal x_0 can be correctly decoded at the second stage of SIC ($x_{\ell,1} \rightarrow x_0 \rightarrow x_{\ell,2}$) subject to the constraints $R_{\ell,1} > \hat{R}_{\ell,1}$ and $R_{\ell,2} \leq \log_2(1 + \hat{\tau})$. Thus, the admitted GFU's achievable rate $R_\ell = R_{\ell,1} + R_{\ell,2}$ can be maximized by first maximizing $R_{\ell,2} = \log_2(1 + \gamma_{\ell,2})$, which is obtained

as $R_{\ell,2} = \log_2(1+\hat{\tau})$ by setting $\gamma_{\ell,2} = \hat{\tau}$. The corresponding optimal transmit power allocation factor is given by

$$\alpha^* = 1 - \frac{\hat{\tau}}{P_s|h_\ell|^2}. \tag{13}$$

By setting the target rate $\hat{R}_{\ell,2} = \log_2(1+\hat{\tau})$ to transmit $x_{\ell,2}$, the optimal target rate allocation factor is given by

$$\beta^* = 1 - \frac{\log_2(1+\hat{\tau})}{\hat{R}_s}. \tag{14}$$

Furthermore, $R_{\ell,1}$ can be maximized by setting $\ell = K$ considering that U_K has the greatest channel gain, i.e., the achievable rate for the GFU is maximized by admitting U_K. Accordingly, the optimal transmit power and target rate allocation factors are respectively given by $\alpha^*(K)$ and β^*, and the achievable rate in this case can be written as

$$R_K^{(\text{II})} = R_{K,1}^{(\text{II})} + R_{K,2}^{(\text{II})}, \tag{15}$$

where

$$R_{K,1}^{(\text{II})} = \log_2\left(1 + \frac{P_s|h_K|^2 - \hat{\tau}}{P_0|h_0|^2 + \hat{\tau} + 1}\right) \tag{16}$$

and

$$R_{K,2}^{(\text{II})} = \log_2(1+\hat{\tau}). \tag{17}$$

Since the received SINR/SNR $\gamma_0(\alpha^*(K))$ and $\gamma_{K,2}(\alpha^*(K))$ provide the necessary conditions for the correct decoding of x_0 and $x_{K,2}$ in SIC processing $x_{K,1} \to x_0 \to x_{K,2}$, only the failure decoding of $x_{K,1}$ can result in error propagation in SIC. To avoid this error propagation, $R_{K,1}^{(\text{II})} \geq \hat{R}_{s,1}$ is required to decode $x_{K,1}$ correctly or equivalently $R_K^{(\text{II})} \geq \hat{R}_s$; Otherwise, both U_0 and U_K encounter outage. Therefore, in the RSMA-SGF scheme, U_K is permitted to transmit only when $R_{K,1}^{(\text{II})} \geq \hat{R}_{s,1}$; Otherwise, U_K keeps silence while U_0 is transmitting alone to the BS.

Case III: $\tau = 0$. In this case, it can be seen that $\hat{\tau} < 0$, so that x_0 cannot be correctly decoded due to a weak channel gain $|h_0|^2$. To avoid error propagation in SIC processing $x_{\ell,1} \to x_0 \to x_{\ell,2}$ caused by the failure decoding of x_0, the admitted GFU is chosen not to transmit $x_{\ell,2}$ rather to transmit x_ℓ by setting $x_{\ell,1} = x_\ell$ and using the whole P_s. Therefore, the optimal transmit power and target rate allocation factors are given by

$$\alpha^* = 1 \quad \text{and} \quad \beta^* = 1. \tag{18}$$

Since U_K has the greatest channel gain among the GFUs, it is admitted to attain the maximum achievable rate as

$$R_K^{(\text{III})} = \log_2\left(1 + \frac{P_s|h_K|^2}{P_0|h_0|^2 + 1}\right) \tag{19}$$

and the corresponding SIC decoding order $x_{K,1} \to x_0 \to x_{K,2}$ degenerates to $x_K \to x_0$.

Remark 2: Due to the channel gain ordering $|h_1|^2 \leq |h_2|^2 \leq \cdots \leq |h_K|^2$, the maximum achievable rates in Cases I, II, and III for the admitted GFU are always attained by

admitting U_K, no matter which decoding order is applied in SIC. Since the channel coefficients of all the K GFUs follow i.i.d. complex Gaussian distribution, all the GFUs have the equal probability to have the greatest channel gain, or equivalently, to be admitted. Thus, the admission probabilities for all the K GFUs are equal in the RSMA-SGF transmission system.

Remark 3: In Cases I and III, the NOMA-SGF scheme also admits U_K and apply the SIC decoding order $x_0 \to x_K$ and $x_K \to x_0$, respectively, to obtain the maximum achievable rates [6]. Nevertheless, in Case II, the NOMA-SGF scheme admits U_K (or U_k) subject to $P_s|h_1|^2 > \tau$ (or $P_s|h_k|^2 < \tau < P_s|h_{k+1}|^2$). For the NOMA-SGF scheme, the achievable rate of the admitted GFU in Case II is given by [6]

$$R_{\text{NOMA}}^{(\text{II})} = \begin{cases} R_K^{(\text{III})}, & 0 < \tau < P_s|h_1|^2 \\ \max\left\{R_k^{(\text{I})}, R_K^{(\text{III})}\right\}, & P_s|h_k|^2 < \tau < P_s|h_{k+1}|^2 \end{cases}, \tag{20}$$

where $k = 1, 2, \ldots, K-1$. Since $R_K^{(\text{II})} > R_K^{(\text{III})}$ and $R_K^{(\text{II})} > R_k^{(\text{I})}$ ($k = 1, 2, \ldots, K-1$) hold for $\tau > 0$, we have $R_K^{(\text{II})} > R_{\text{NOMA}}^{(\text{II})}$, i.e., the RSMA-SGF scheme always achieves a larger achievable rate for the admitted GFU than that of the NOMA-SGF scheme in Case II.

Remark 4: In Case II, U_K only transmits its signal when $R_{K,1}^{(\text{II})} \geq \hat{R}_{s,1}$, which prevents error propagation in SIC processing $x_{K,1} \to x_0 \to x_{K,2}$. When $R_{K,1}^{(\text{II})} < \hat{R}_{s,1}$, U_K keeps silence and only the GBU U_0 transmits. Thus, the GBU U_0 does not encounter outage when the RSMA-SGF scheme operates in Case II. As such, the outage events occur to the transmissions of x_0 in Cases I and III are the same as in OMA, and the GBU U_0 achieves the same outage performance as in OMA when the RSMA-SGF scheme is applied.

III. OUTAGE PERFORMANCE ANALYSIS

In the RSMA-SGF transmission system, since the GBU's outage performance is guaranteed to be the same as in OMA, we mainly focus on the outage performance of the admitted GFU. In this section, we first introduce the non-outage zone to clarify the advantage of the RSMA-SGF scheme. Then, we derive the analytical expression for the outage probability in closed-form and investigate the asymptotic outage performance in the high SNR region.

For the uplink MACs in which the two-user U_0 and U_K are admitted simultaneously, the non-outage zone is defined by

$$\bar{\mathcal{O}} \triangleq \left\{\left\{\hat{R}_0, \hat{R}_s\right\} \mid \hat{R}_0 \leq R_0, \hat{R}_s \leq R_K\right\}. \tag{21}$$

If a target rate pair $\{\hat{R}_0, \hat{R}_s\}$ lies in the non-outage zone, both U_0 and U_K can attain the achievable rates $R_0 \geq \hat{R}_0$ and $R_K \geq \hat{R}_K$ such that neither U_0 nor U_K encounters the outage event. Otherwise, both U_0 and U_K are in outage. Corresponding to (21), the set $\mathcal{O} \triangleq \{\{\hat{R}_0, \hat{R}_s\} \mid \hat{R}_0 > R_0, \hat{R}_s >$
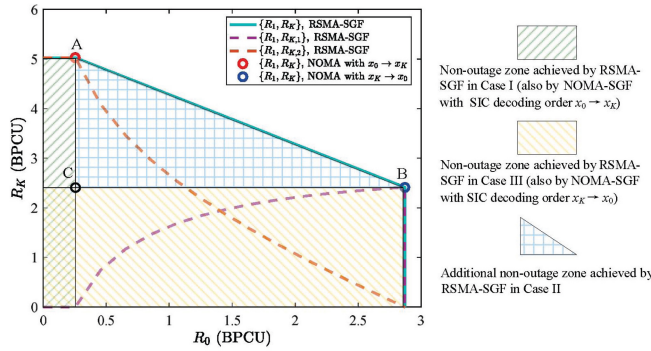
FIGURE 2. Non-outage zones achieved by different schemes ($P_0|h_0|^2 = 8$ dB, $P_s|h_K|^2 = 15$ dB).

R_K} is called the outage zone when both U_0 and U_K are admitted simultaneously.

In Fig. 2, an example of the non-outage zone achieved by the RSMA-SGF scheme is illustrated. For the comparison purpose, the non-outage zone achieved by the NOMA-SGF scheme is also illustrated in which the SIC decoding orders $x_0 \to x_K$ and $x_K \to x_0$ are respectively utilized [6]. In this example, we assume $0 < \tau < P_s|h_1|^2$. From Fig. 2, we can see that the non-outage zones achieved by the NOMA-SGF scheme using the SIC decoding orders $x_0 \to x_K$ and $x_K \to x_0$ are identical to those achieved by the RSMA-SGF scheme in Cases I and III, respectively. Thus, in Cases I and III, the RSMA-SGF scheme can achieve the same outage performance as that of the NOMA-SGF scheme. Nevertheless, the NOMA-SGF scheme cannot prevent U_0 and U_K from being in outage when the target rate pair {$\hat{R}_0, \hat{R}_K$} lies in the triangle ABC, which is beyond the non-outage zone of the NOMA-SGF scheme. Fortunately, the points on the line AB in Fig. 2 can be achieved by rate-splitting. Specifically, an additional non-outage zone, the triangle ABC, is achieved when the RSMA-SGF scheme operates in Case II. Thus, the non-outage zone of the RSMA-SGF scheme is extended compared to that of the NOMA-SGF scheme, which shows that the RSMA-SGF scheme can support more target rate pairs than that of the NOMA-SGF scheme.

With respect to the operations of the RSMA-SGF scheme in Cases I, II, and III, the outage probability of the admitted GFU can be written as

$$P_{\text{out}} = P_{\text{out}}^{(\text{I})} + P_{\text{out}}^{(\text{II})} + P_{\text{out}}^{(\text{III})}, \tag{22}$$

where $P_{\text{out}}^{(\text{I})}$, $P_{\text{out}}^{(\text{II})}$, and $P_{\text{out}}^{(\text{III})}$ respectively denote the probability of that U_K encounters outage in Cases I, II, and III, which can be expressed as

$$P_{\text{out}}^{(\text{I})} = \Pr\left(0 < P_s|h_K|^2 < \tau, R_K^{(\text{I})} < \hat{R}_s\right), \tag{23}$$

$$P_{\text{out}}^{(\text{II})} = \sum_{k=0}^{K-1} P_{\text{out}}^{(\text{II},k)} \tag{24}$$

and

$$P_{\text{out}}^{(\text{III})} = \Pr\left(\tau = 0, R_K^{(\text{III})} < \hat{R}_s\right), \tag{25}$$

with

$$P_{\text{out}}^{(\text{II},0)} = \Pr\left(0 < \tau < P_s|h_1|^2, R_K^{(\text{II})} < \hat{R}_s\right) \tag{26}$$

and for $k = 1, 2, \ldots, K-1$,

$$P_{\text{out}}^{(\text{II},k)} = \Pr\left(P_s|h_k|^2 < \tau < P_s|h_{k+1}|^2, R_K^{(\text{II})} < \hat{R}_s\right). \tag{27}$$

The following theorem provides an exact expression for the admitted GFU's outage probability achieved by the RSMA-SGF scheme.

Theorem 1: Assume that $K \geq 2$, the outage probability of the admitted GFU is given by

$$
\begin{aligned}
P_{\text{out}} = {} & \frac{\varphi_0}{K(K-1)} \sum_{n=0}^{K} \binom{K}{n}(-1)^n \mu_1 \nu(0, \mu_2) \\
& + \sum_{k=1}^{K-2} \varphi_k \sum_{m=0}^{K-k} \binom{K-k}{m}(-1)^m \\
& \times \sum_{n=0}^{k} \binom{k}{n}(-1)^n e^{\frac{n}{P_s}} \mu_3 \nu(n, \mu_4) \\
& + \frac{\varphi_0}{K-1} \sum_{n=0}^{K-1} \binom{K-1}{n}(-1)^n e^{\frac{n}{P_s}} \\
& \times \left(e^{\frac{1}{P_s}} \nu(n, \mu_5) - e^{-\frac{\varepsilon_0 + \varepsilon_s + \varepsilon_0 \varepsilon_s}{P_s}} \nu(n, \mu_6)\right) \\
& + \sum_{n=0}^{K} \binom{K}{n}(-1)^n e^{\frac{n}{P_s}} \nu(n, 0) \\
& + \left(1 - e^{-\eta_s}\right)^K e^{-\eta_0(1 + \varepsilon_s)} \\
& + \sum_{n=0}^{K} \binom{K}{n}(-1)^n e^{-n\eta_s} \frac{1 - e^{-(1 + n\eta_s P_0)\eta_0}}{1 + n\eta_s P_0}, \tag{28}
\end{aligned}
$$

where $\binom{K}{n}$ denotes the binomial coefficient, $\varepsilon_s \triangleq 2^{\hat{R}_s} - 1$, $\eta_0 \triangleq \frac{\varepsilon_0}{P_0}$, $\eta_s \triangleq \frac{\varepsilon_s}{P_s}$, $\mu_1 = e^{\frac{K-n(1+\varepsilon_0)(1+\varepsilon_s)}{P_s}}$, $\mu_2 = \frac{K-n}{P_s \eta_0} - \frac{nP_0}{P_s}$, $\mu_3 = e^{\frac{K-k-m(1+\varepsilon_0)(1+\varepsilon_s)}{P_s}}$, $\mu_4 = \frac{K-k-m}{P_s \eta_0} - \frac{mP_0}{P_s}$, $\mu_5 = \frac{1}{P_s \eta_0}$, $\mu_6 = -\frac{P_0}{P_s}$, $\varphi_0 = \frac{K!}{(K-2)!}$, $\varphi_k = \frac{K!}{k!(K-k)!}$ for $1 \leq k \leq K-2$, and

$$
\nu(n, \mu) =
\begin{cases}
\varepsilon_s \eta_0, & \text{if } \mu = -1 - \frac{n}{P_s \eta_0}, \\
\dfrac{e^{-\eta_0\left(\frac{n}{P_s \eta_0} + \mu + 1\right)} - e^{-\eta_0(1+\varepsilon_s)\left(\frac{n}{P_s \eta_0} + \mu + 1\right)}}{\frac{n}{P_s \eta_0} + \mu + 1}, & \\
& \text{otherwise.}
\end{cases} \tag{29}
$$

Proof: See Appendix A. ∎

Remark 5: In deriving the expressions for $P_{\text{out}}^{(\text{I})}$ and $P_{\text{out}}^{(\text{II})}$, as derived in Appendix A, all the outage events reflect the fact that the upper bound on the channel gain $|h_K|^2$ should be greater than the lower bound on a specific GFU's channel gain, which is always and naturally guaranteed by $|h_0|^2 < \eta_0(1 + \varepsilon_s)$ without imposing additional constraints on ε_0 and
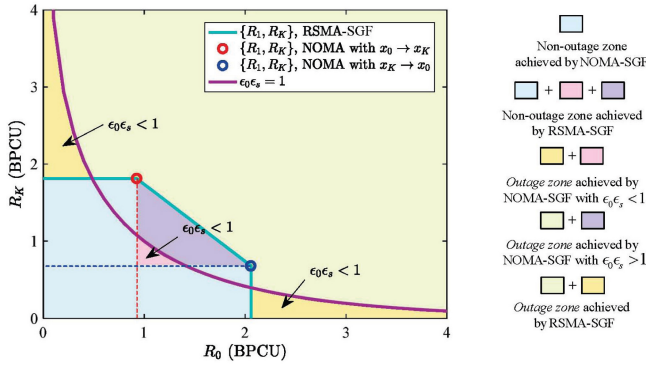
FIGURE 3. Outage and non-outage zones achieved by different schemes $(P_0|h_0|^2 = 5$ dB, $P_s|h_K|^2 = 4$ dB).

ε_s, so that the derived expression for the outage probability is applicable to all the feasible ε_0 and ε_s. On the contrary, for the NOMA-SGF scheme, the analytical expression for the outage probability in [6] is applicable only for $\varepsilon_0 \varepsilon_s < 1$. As an example, the outage and non-outage zones achieved by the RSMA-SGF and the NOMA-SGF schemes are illustrated in Fig. 3. It can be seen that the outage zone constrained by $\varepsilon_0 \varepsilon_s < 1$ is a small portion of the whole outage zone for the NOMA-SGF scheme and a similar phenomenon happens to the RSMA-SGF scheme as well. Therefore, the analytical results provided in Theorem 1 are more general due to its applicability to all the feasible values of ε_0 and ε_s. In contrast to the RSMA-SGF scheme, the NOMA-SGF scheme results in a worse outage performance due to the extended outage zone.

When the considered system consists of a single GFU and GBU, the two users are paired directly. Then, the GFU's outage probability achieved by the RSMA-SGF scheme can be written as:

$$
\begin{aligned}
P_{\text{out}} = & \Pr\left(0 < P_s|h_1|^2 \le \tau, R_1^{(\mathrm{I})} < \hat{R}_s\right) \\
& + \Pr\left(0 < \tau < P_s|h_1|^2, R_1^{(\mathrm{II})} < \hat{R}_s\right) \\
& + \Pr\left(\tau = 0, R_1^{(\mathrm{III})} < \hat{R}_s\right).
\end{aligned}
\tag{30}
$$

Corollary 1: Assume that $K = 1$, the admitted GFU's outage probability is given by

$$
\begin{aligned}
P_{\text{out}} = & 1 - e^{-\frac{\varepsilon_0 + \varepsilon_s + \varepsilon_0 \varepsilon_s}{P_s}} \nu(0, \mu_6) - e^{-\eta_s - \eta_0(1+\varepsilon_s)} \\
& - \frac{e^{-\eta_s}\left(1 - e^{-\eta_0 - \varepsilon_0 \eta_s}\right)}{1 + P_0 \eta_s}
\end{aligned}
\tag{31}
$$

and its approximation in the high SNR region is given by

$$
P_{\text{out}} \approx \frac{\varepsilon_s}{P_s}.
\tag{32}
$$

Proof: A proof can be found in [15]. ∎

Corollary 2: Assuming that $K \ge 2$, the outage probability experienced by the admitted GFU can be approximated in the high SNR region as follows:

$$
P_{\text{out}} \approx \frac{\varphi_0 \varepsilon_0 (1 + \varepsilon_0)^K}{P_s^{K+1} K(K-1)}
$$

$$
\times \sum_{n=0}^{K} \binom{K}{n} \frac{(-1)^n}{n+1}\left((1+\varepsilon_s)^{K+1} - (1+\varepsilon_s)^{K-n}\right)
$$

$$
+ \frac{\varphi_k \varepsilon_0 (1+\varepsilon_0)^{K-k}(-1)^k}{P_s^{K+1}}
$$

$$
\times \sum_{m=0}^{K-k} \binom{K-k}{m} (-1)^m (1+\varepsilon_s)^{K-k-m}
$$

$$
\times \sum_{n=0}^{k} \binom{k}{n} (-1)^n \frac{(1+\varepsilon_s)^{m+n+1} - 1}{m+n+1}
$$

$$
+ \frac{\varphi_0 \varepsilon_0 \varepsilon_s^K (1+\varepsilon_0)(1+\varepsilon_s)}{P_s^{K+1} K(K-1)}
$$

$$
- \frac{\varphi_0 \varepsilon_s^K \left(\varepsilon_0^{-1} + 1\right)(K(1+\varepsilon_s)+1)}{P_s^{K+1} K(K-1)(K+1)}
$$

$$
+ \frac{\varepsilon_0 \varepsilon_s^{K+1}}{(K+1)P_s^{K+1}} + \frac{\varepsilon_s^K}{P_s^K} - \frac{\varepsilon_0 \varepsilon_s^K (1+\varepsilon_s)}{P_s^{K+1}}
$$

$$
+ \frac{\varepsilon_s^K \left((1+\varepsilon_0)^{K+1} - 1\right)}{P_s^{K+1}(K+1)}
$$

$$
- \frac{\varepsilon_s^K \left((\varepsilon_0(K+1)-1)(1+\varepsilon_0)^{K+1}+1\right)}{P_s^{K+2}(K+2)(K+1)}.
\tag{33}
$$

Proof: See Appendix B. ∎

From the results in Corollary 2, we can see that there is one term in (33) being proportional to $\frac{1}{P_s^K}$, while the other terms are proportional to $\frac{1}{P_s^{K+1}}$ or $\frac{1}{P_s^{K+2}}$. Based on the results of Corollaries 1 and 2, we have the following corollary.

Corollary 3: Assuming that $K \ge 1$, the admitted GFU's outage probability can be approximated as

$$
P_{\text{out}} \approx \frac{\varepsilon_s^K}{P_s^K}
\tag{34}
$$

in the high SNR region. Thus, a diversity gain of K is achieved by the RSMA-SGF scheme.

Remark 6: Corollaries 2 and 3 demonstrate that the RSMA-SGF scheme ensures an achievable diversity gain proportional to the number of the GFUs without resulting in an outage floor.

IV. SIMULATION RESULTS
In this section, we present simulation results to verify the accuracy of the analytical results and the superior outage performance of the RSMA-SGF scheme. For the purpose of comparisons, the admitted GFU's outage probabilities achieved by the NOMA-SGF scheme [6] and the NOMA-SGF scheme with power control (NOMA-SGF-PC) [13] are also presented. In the simulation, the channel coefficients are randomly generated according to i.i.d. circular symmetric complex Gaussian random distribution with zero mean and unit variance and the transmission data rate is measured in bits per channel use (BPCU).

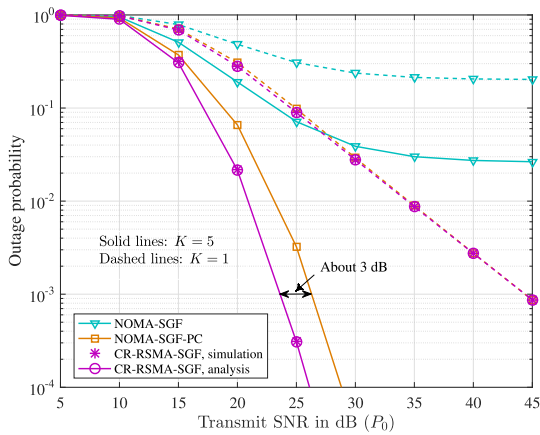The outage performance achieved by the RSMA-SGF scheme is compared with those of the NOMA-SGF and

FIGURE 4. Outage probability comparison of the SGF schemes with $\hat{R}_0 = 2.5$ BPCU, $\hat{R}_s = 1.5$ BPCU, and $P_s = \frac{P_0}{15}$.
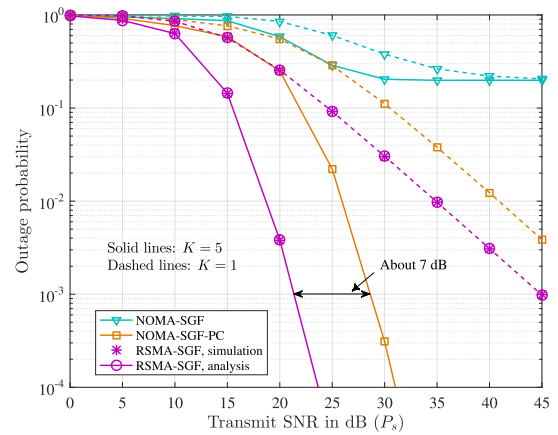

FIGURE 5. Outage probability comparison of the SGF schemes with $\hat{R}_0 = 3$ BPCU, $\hat{R}_s = 3$ BPCU, and the fixed $P_0 = 15$ dB.

NOMA-SGF-PC schemes in Fig. 4, where we set $\hat{R}_0 = 2.5$ BPCU, $\hat{R}_s = 1.5$ BPCU, and $P_s = \frac{P_0}{15}$, i.e., the transmit SNR of U_0 is 11.76 dB higher than that of the GFUs. From Fig. 4, we can see that the RSMA-SGF scheme achieves the smallest outage probabilities among the three schemes for both $K = 1$ and $K = 5$. The results in Fig. 4 also verify the accuracy of the derived analytical expressions. As transmit SNR increases, the outage probabilities achieved by both the RSMA-SGF and NOMA-SGF-PC schemes decrease monotonically, whereas an outage probability floor occurs for the NOMA-SGF scheme in the high SNR regime. The reason for the outage probability floor is that the achievable rate attained by the NOMA-SGF scheme satisfies $R_{\text{NOMA}}^{(II)} = R_K^{(III)} \to \log_2(1 + P_s/P_0)$ as $P_s \to \infty$ and $P_0 \to \infty$ under the condition of $0 < \tau < P_s|h_1|^2$ in Case II, which always results in an outage event if $\log_2(1 + P_s/P_0) < \hat{R}_s$ occurs. Although the NOMA-SGF-PC scheme avoids the outage probability floor, the achieved outage probability is still higher than that of the RSMA-SGF scheme. At the outage probability level of 10^{-3}, the RSMA-SGF scheme achieves a 3 dB transmit SNR gain over that of the NOMA-SGF-PC scheme. Therefore, the results in Fig. 4 verify that the RSMA-SGF scheme achieves the superior outage performance compared to the NOMA-SGF and NOMA-SGF-PC schemes.

In Fig. 5, we investigate the outage performance achieved by the SGF schemes for various transmit powers. In particular, we set a fixed transmit power $P_0 = 15$ dB and vary P_s from 0 dB to 45 dB, which reflects that the GFUs can have greater and lower transmit SNRs than that of U_0. The results in Fig. 5 also verify the accuracy of the derived analytical expressions. From Fig. 5, we can see that the RSMA-SGF scheme achieves the smallest outage probabilities in the whole SNR region. At the outage probability level of 10^{-3}, the RSMA-SGF scheme achieves a 7 dB transmit SNR gain over that of the NOMA-SGF-PC scheme. As transmit SNR increases, the outage probability achieved by the RSMA-SGF scheme decreases monotonically for both
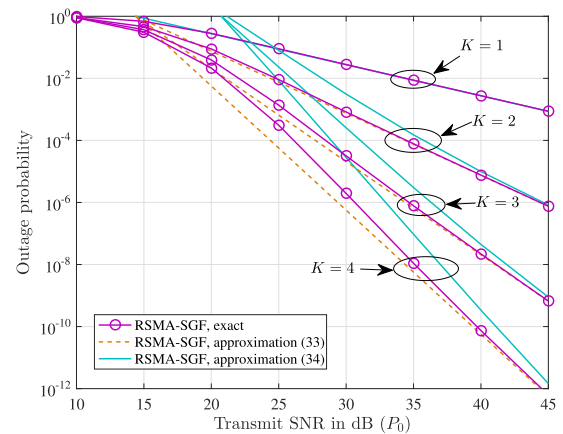

FIGURE 6. Accuracy of the derived analytical expressions.

$K = 1$ and $K = 5$. Also, the NOMA-SGF scheme achieves the worst outage probabilities in the whole SNR region. Especially in the high SNR region, the outage probability floor occurs for the NOMA-SGF scheme due to a limited asymptotic achievable rate $R_{\text{NOMA}}^{(II)}$ as resulted by (20). The results in Fig. 5 verify that the superior outage performance of the RSMA-SGF scheme is irrespective of whether the GFUs are stronger users or weaker users compared to U_0.

In Fig. 6, we examine the accuracy of the derived analytical expressions for the outage probability. In Fig. 6, we set $\hat{R}_0 = 2$ BPCU, $\hat{R}_s = 1.5$ BPCU, and $P_s = \frac{P_0}{15}$. In Fig. 6, for the curves corresponding to the expressions provided in Corollaries 2 and 3, we denote them by "approximation (33)" and "approximation (34)", respectively. The curves in Fig. 6 verify that the accuracy of derived analytical expression in Theorem 1. For the approximated expressions, we can see that the curves of the "approximation (33)" match well with the exact results in the high SNR region, whereas the curves of the "approximation (34)" match well with the exact results in the high SNR region only for small K values. For large K values ($K = 4$ in this example), a gap exists between the curves of the "approximation (34)" and exact results. The
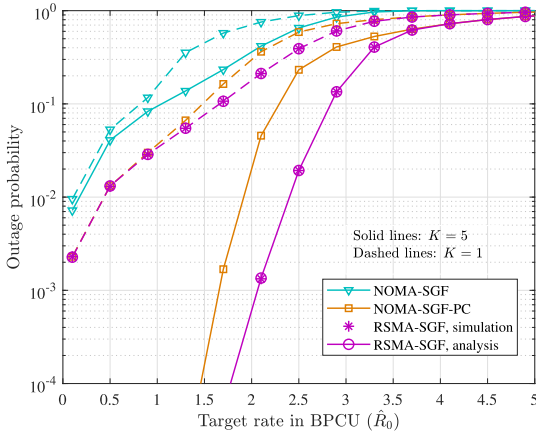
FIGURE 7. Impact of the target rate on the outage probability.
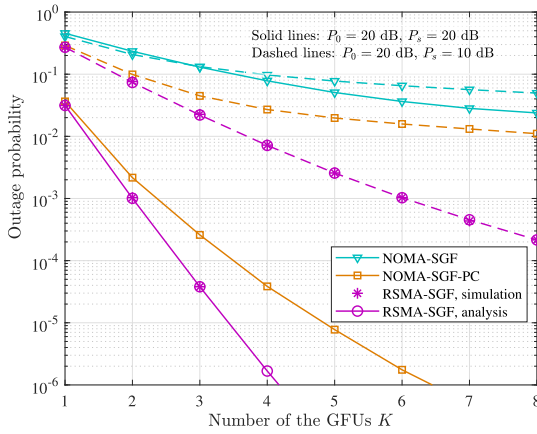
FIGURE 8. Impact of the number of the GFUs on the outage probability ($\hat{R}_0 = 1.5$ BPCU and $\hat{R}_s = 2$ BPCU).

reason for this phenomenon is that we ignore the terms being proportional to $\frac{1}{P_s^{K+1}}$ and $\frac{1}{P_s^{K+2}}$ in the expression in (34).

The impact of the target rate on the outage probability is investigated in Fig. 7. For the simulation results in Fig. 7, we set $P_0 = 10$ dB, $P_s = 15$ dB, and $\hat{R}_0 = \hat{R}_s$. It is seen in Fig. 7 that for given transmit SNR values, the RSMA-SGF scheme achieves the smallest outage probabilities in the considered whole target rate region. As the target rate increases, the outage probability values achieved by all the SGF schemes increase and approach 1.

The impact of the number of the GFUs on the outage probability is investigated in Fig. 8. For the simulation corresponding to Fig. 8, we set $\{\hat{R}_0 = 1.5$ BPCU, $\hat{R}_s = 2$ BPCU$\}$ and consider two cases of transmit SNR settings $\{P_0 = 20$ dB, $P_s = 10$ dB$\}$ and $\{P_0 = 20$ dB, $P_s = 10$ dB$\}$. As K increases, the outage probabilities achieved by the three SGF schemes decreases. Furthermore, Fig. 8 verifies that the multiuser diversity is achieved by the RSMA-SGF scheme. Consequently, among the three SGF schemes, the RSMA-SGF scheme achieves the smallest outage probability for different numbers of the GFUs.

V. CONCLUSION

In this paper, we have conducted the outage performance analysis for the RSMA-SGF transmission system. By applying rate-splitting under the CR principle, the RSMA-SGF scheme effectively utilizes the transmit power to attain the maximum achievable rate for the admitted GFU. Without introducing intolerable interference to the GBU, the RSMA-SGF scheme has significantly extended the non-outage zone compared to the NOMA-SGF scheme. We have derived exact and approximated expressions for the outage probability of the admitted GFU and revealed that the full multiuser diversity gain can be achieved by the RSMA-SGF scheme. Simulation results have verified the superior outage performance achieved by the RSMA-SGF scheme.

APPENDIX A
PROOF OF THEOREM 1

To derive the admitted GFU's outage probability, we evaluate the probability terms $P_{\text{out}}^{(\text{I})}$, $P_{\text{out}}^{(\text{II})}$, and $P_{\text{out}}^{(\text{III})}$, respectively. In Case II, $P_{\text{out}}^{(\text{II})} = \sum_{k=0}^{K-1} P_{\text{out}}^{(\text{II},k)}$ is derived by evaluating the different $P_{\text{out}}^{(\text{II},k)}$ taking into account the corresponding order statistics.

A. EVALUATION OF $P_{OUT}^{(II,0)}$

To evaluate $P_{\text{out}}^{(\text{II},0)}$, let us introduce S_0 as

$$S_0 = \Pr\left(|h_1|^2 > \frac{P_0 \varepsilon_0^{-1} |h_0|^2 - 1}{P_s}, \right.$$
$$\left. |h_K|^2 < \frac{(1+\varepsilon_s)(1+\varepsilon_0) - \left(1 + P_0|h_0|^2\right)}{P_s}\right). \text{ (A.1)}$$

Then, $P_{\text{out}}^{(\text{II},0)}$ in (26) can be rewritten as

$$P_{\text{out}}^{(\text{II},0)} = \mathbb{E}_{\eta_0 < |h_0|^2 < \eta_0(1+\varepsilon_s) + \frac{\varepsilon_s}{P_0}} \{S_0\}, \quad \text{(A.2)}$$

where $\varepsilon_s = 2^{\hat{R}_s} - 1$ and $\eta_0 = \frac{\varepsilon_0}{P_0}$. In (A.2), the expectation on S_0 is conducted over $\eta_0 < |h_0|^2 < \eta_0(1+\varepsilon_s) + \frac{\varepsilon_s}{P_0}$ taking into account $\hat{\tau} > 0$ and $\frac{(1+\varepsilon_s)(1+\varepsilon_0)-(1+P_0|h_0|^2)}{P_s} > 0$. Since the upper bound on $|h_K|^2$ should be larger than the lower bound on $|h_1|^2$, the expectation in (A.2) should consider the hidden constraint $|h_0|^2 < \eta_0(1 + \varepsilon_s)$ as well, so that $P_{\text{out}}^{(\text{II},0)}$ is rewritten as

$$P_{\text{out}}^{(\text{II},0)} = \mathbb{E}_{\eta_0 < |h_0|^2 < \eta_0(1+\varepsilon_s)} \{S_0\}. \quad \text{(A.3)}$$

The joint probability density function (PDF) of the order statistics $|h_1|^2$ and $|h_K|^2$ is given by [44]

$$f_{|h_1|^2, |h_K|^2}(x, y) = \varphi_0 e^{-x}\left(e^{-x} - e^{-y}\right)^{K-2} e^{-y}, \quad \text{(A.4)}$$

where $x < y$ and $\varphi_0 = \frac{K!}{(K-2)!}$. Then, S_0 can be evaluated as follows:

$$S_0 = \varphi_0 \sum_{i=0}^{K-2} \binom{K-2}{i} (-1)^i$$

$$\times \int_{\frac{\eta_0^{-1}|h_0|^2-1}{P_s}}^{\frac{(1+\varepsilon_s)(1+\varepsilon_0)-(1+P_0|h_0|^2)}{P_s}} e^{-(K-i-1)x}$$

$$\times \int_{x}^{\frac{(1+\varepsilon_s)(1+\varepsilon_0)-(1+P_0|h_0|^2)}{P_s}} e^{-(i+1)y} dy\,dx$$

$$= \varphi_0 \sum_{i=0}^{K-2} \binom{K-2}{i} \frac{(-1)^i}{i+1}$$

$$\times \left(\frac{\tilde{\mu}_3 e^{-\tilde{\mu}_4|h_0|^2} - \tilde{\mu}_5 e^{-\tilde{\mu}_6|h_0|^2}}{K} \right.$$

$$\left. - \frac{\tilde{\mu}_1 e^{-\tilde{\mu}_2|h_0|^2} - \tilde{\mu}_5 e^{-\tilde{\mu}_6|h_0|^2}}{K-i-1} \right), \quad (A.5)$$

where $\tilde{\mu}_1 = e^{\frac{K-(1+i)(1+\varepsilon_0)(1+\varepsilon_s)}{P_s}}$, $\tilde{\mu}_2 = \frac{K-i-1}{P_s\eta_0} - \frac{P_0(1+i)}{P_s}$, $\tilde{\mu}_3 = e^{\frac{K}{P_s}}$, $\tilde{\mu}_4 = \frac{K}{P_s\eta_0}$, $\tilde{\mu}_5 = e^{-\frac{K(\eta_0+\eta_s+\eta_0\eta_s)}{P_s}}$, $\tilde{\mu}_6 = -\frac{KP_0}{P_s}$, and $\eta_s = \frac{\varepsilon_s}{P_s}$.

Next, we introduce a term $\nu(i, \mu)$ as follows:

$$\nu(i, \mu) \triangleq \mathop{\mathbb{E}}_{\eta_0 < |h_0|^2 < \eta_0(1+\varepsilon_s)} \left\{ e^{-\left(\frac{i}{P_s\eta_0}+\mu\right)|h_0|^2} \right\}$$

$$= \int_{\eta_0}^{\eta_0(1+\varepsilon_s)} e^{-\left(\frac{i}{P_s\eta_0}+\mu+1\right)x} dx$$

$$= \begin{cases} \varepsilon_s\eta_0, & \text{if } \mu = -1 - \frac{i}{P_s\eta_0}, \\ \frac{e^{-\eta_0\left(\frac{i}{P_s\eta_0}+\mu+1\right)} - e^{-\eta_0(1+\varepsilon_s)\left(\frac{i}{P_s\eta_0}+\mu+1\right)}}{\frac{i}{P_s\eta_0}+\mu+1}, \\ & \text{otherwise.} \end{cases} \quad (A.6)$$

By substituting (A.6) into (A.5), $P_{\text{out}}^{(\text{II},0)}$ can be evaluated as

$$P_{\text{out}}^{(\text{II},0)} = \varphi_0 \sum_{i=0}^{K-2} \binom{K-2}{i} \frac{(-1)^i}{i+1} \left(\frac{\tilde{\mu}_3\nu(0,\tilde{\mu}_4) - \tilde{\mu}_5\nu(0,\tilde{\mu}_6)}{K} \right.$$

$$\left. - \frac{\tilde{\mu}_1\nu(0,\tilde{\mu}_2) - \tilde{\mu}_5\nu(0,\tilde{\mu}_6)}{K-i-1} \right)$$

$$\stackrel{(a)}{=} \frac{\varphi_0}{1-K} \sum_{n=0}^{K-1} \binom{K-1}{n} (-1)^n \left(\frac{\tilde{\mu}_3\nu(0,\tilde{\mu}_4) - \tilde{\mu}_5\nu(0,\tilde{\mu}_6)}{K} \right.$$

$$\left. - \frac{\mu_1\nu(0,\mu_2) - \tilde{\mu}_5\nu(0,\tilde{\mu}_6)}{K-n} \right), \quad (A.7)$$

where $\mu_1 = e^{\frac{K-n(1+\varepsilon_0)(1+\varepsilon_s)}{P_s}}$ and $\mu_2 = \frac{K-n}{P_s\eta_0} - \frac{P_0 n}{P_s}$. In step (a) of (A.7), we have applied $\binom{K-2}{i} = \binom{K-1}{i+1}\frac{i+1}{K-1}$, replaced $n = i+1$, and added the term for $n = 0$ without changing the summation since $\frac{\tilde{\mu}_3\nu(0,\tilde{\mu}_4)-\tilde{\mu}_5\nu(0,\tilde{\mu}_6)}{K} - \frac{\mu_1\nu(0,\mu_2)-\tilde{\mu}_5\nu(0,\tilde{\mu}_6)}{K-n} = 0$ when $n = 0$.

By eliminating the terms that are independent of n using $\sum_{n=0}^{K-1} \binom{K-1}{n}(-1)^n = 0$, (A.7) can be simplified as:

$$P_{\text{out}}^{(\text{II},0)} = \frac{\varphi_0}{K-1} \sum_{n=0}^{K-1} \binom{K-1}{n} (-1)^n$$

$$\times \frac{\mu_1\nu(0,\mu_2) - \tilde{\mu}_5\nu(0,\tilde{\mu}_6)}{K-n}$$

$$= \frac{\varphi_0}{K(K-1)} \sum_{n=0}^{K} \binom{K}{n} (-1)^n$$

$$\times (\mu_1\nu(0,\mu_2) - \tilde{\mu}_5\nu(0,\tilde{\mu}_6)), \quad (A.8)$$

where the term for $n = K$ is added without changing the summation since $\mu_1\nu(0,\mu_2) - \tilde{\mu}_5\nu(0,\tilde{\mu}_6) = 0$ when $n = K$. Again, by eliminating the terms that are independent of n using $\sum_{n=0}^{K} \binom{K}{n}(-1)^n = 0$, $P_{\text{out}}^{(\text{II},0)}$ can be further simplified as:

$$P_{\text{out}}^{(\text{II},0)} = \frac{\varphi_0}{K(K-1)} \sum_{n=0}^{K} \binom{K}{n} (-1)^n \mu_1\nu(0,\mu_2). \quad (A.9)$$

B. EVALUATION OF $P_{OUT}^{(II,K)}$ WITH $1 \leq K \leq K-2$

When $1 \leq k \leq K-2$, three order statistics, h_k, h_{k+1}, and h_K, are involved in $P_{\text{out}}^{(\text{II},k)}$, which can be rewritten as:

$$P_{\text{out}}^{(\text{II},k)} = \Pr\left(|h_0|^2 > \eta_0, |h_k|^2 < \frac{\tau}{P_s}, |h_{k+1}|^2 > \frac{\tau}{P_s}, R_{\text{II},K} < \hat{R}_k \right)$$

$$= \mathop{\mathbb{E}}_{\eta_0 < |h_0|^2 < \eta_0(1+\varepsilon_s)} \{S_k\}, \quad (A.10)$$

where S_k is defined by

$$S_k \triangleq \Pr\left(|h_k|^2 < \frac{P_0\varepsilon_0^{-1}|h_0|^2 - 1}{P_s}, |h_{k+1}|^2 > \frac{P_0\varepsilon_0^{-1}|h_0|^2 - 1}{P_s}, \right.$$

$$\left. |h_K|^2 < \frac{(1+\varepsilon_s)(1+\varepsilon_0) - (1+P_0|h_0|^2)}{P_s} \right). \quad (A.11)$$

In (A.10), the expectation is taken over $\eta_0 < |h_0|^2 < \eta_0(1+\varepsilon_s)$ considering the relationship between the upper and lower bounds on the channel gains.

The joint PDF of three order statistics, h_k, h_{k+1}, and h_K, is given by [44]

$$f_{|h_k|^2, |h_{k+1}|^2, |h_K|^2}(x, y, z)$$

$$= \tilde{\varphi}_k e^{-x} (1-e^{-x})^{k-1} e^{-y} (e^{-y} - e^{-z})^{K-k-2} e^{-z}$$

$$= \tilde{\varphi}_k \sum_{i=0}^{K-k-2} \binom{K-k-2}{i} (-1)^i e^{-x} (1-e^{-x})^{k-1}$$

$$\times e^{-(K-k-i-1)y} e^{-(i+1)z}, \quad (A.12)$$

where $x \leq y \leq z$ and $\tilde{\varphi}_k = \frac{K!}{(k-1)!(K-k-2)!}$. Using (A.12), S_k can be expressed in terms of $|h_0|^2$ as follows:

$$S_k = \tilde{\varphi}_k \sum_{i=0}^{K-k-2} \binom{K-k-2}{i} (-1)^i$$

$$\times \int_0^{\frac{\eta_0^{-1}|h_0|^2-1}{P_s}} e^{-x}\left(1-e^{-x}\right)^{k-1}$$

$$\times \int_{\frac{\eta_0^{-1}|h_0|^2-1}{P_s}}^{\frac{(1+\varepsilon_s)(1+\varepsilon_0)-\left(1+P_0|h_0|^2\right)}{P_s}} e^{-(K-k-i-1)y}$$

$$\times \int_y^{\frac{(1+\varepsilon_s)(1+\varepsilon_0)-\left(1+P_0|h_0|^2\right)}{P_s}} e^{-(i+1)z} dzdydx. \quad (A.13)$$

After some algebraic manipulations, S_k can be further evaluated as follows:

$$S_k = \tilde{\varphi}_k \sum_{i=0}^{K-k-2} \binom{K-k-2}{i} \sum_{\ell=0}^{k} \binom{k}{\ell} \frac{(-1)^{\ell+i} e^{\frac{\ell}{P_s}} e^{-\frac{\ell|h_0|^2}{P_s \eta_0}}}{k(i+1)}$$

$$\times \left(\frac{\tilde{\mu}_1 e^{-\tilde{\mu}_2|h_0|^2} - \tilde{\mu}_5 e^{-\tilde{\mu}_6|h_0|^2}}{K-k} - \frac{\tilde{\mu}_3 e^{-\tilde{\mu}_4|h_0|^2} - \tilde{\mu}_5 e^{-\tilde{\mu}_6|h_0|^2}}{K-k-i-1}\right),$$
(A.14)

where $\tilde{\mu}_1 = e^{\frac{K-k}{P_s}}$, $\tilde{\mu}_2 = \frac{K-k}{P_s \eta_0}$, $\tilde{\mu}_3 = e^{\frac{K-k-(1+i)(1+\varepsilon_0)(1+\varepsilon_s)}{P_s}}$, $\tilde{\mu}_4 = \frac{K-k-i-1}{P_s \eta_0} - \frac{(1+i)P_0}{P_s}$, $\tilde{\mu}_5 = e^{-\frac{(K-k)(\varepsilon_0+\varepsilon_s+\varepsilon_0\varepsilon_s)}{P_s}}$, and $\tilde{\mu}_6 = -\frac{(K-k)P_0}{P_s}$.

By substituting (A.14) into (A.10), $P_{\text{out}}^{(\text{II},k)}$ can be evaluated as:

$$P_{\text{out}}^{(\text{II},k)} = \tilde{\varphi}_k \sum_{i=0}^{K-k-2} \binom{K-k-2}{i} \frac{(-1)^i}{k(i+1)} \sum_{n=0}^{k} \binom{k}{n} (-1)^n e^{\frac{n}{P_s}}$$

$$\times \left(\frac{\tilde{\mu}_1 \nu(n,\tilde{\mu}_2) - \tilde{\mu}_5 \nu(n,\tilde{\mu}_6)}{K-k}\right.$$

$$\left. - \frac{\tilde{\mu}_3 \nu(n,\tilde{\mu}_4) - \tilde{\mu}_5 \nu(n,\tilde{\mu}_6)}{K-k-i-1}\right)$$

$$\stackrel{(b)}{=} \frac{-\tilde{\varphi}_k}{k(K-k-1)} \sum_{m=0}^{K-k-1} \binom{K-k-1}{m} (-1)^m$$

$$\times \sum_{n=0}^{k} \binom{k}{n} (-1)^n e^{\frac{n}{P_s}} \left(\frac{\tilde{\mu}_1 \nu(n,\tilde{\mu}_2) - \tilde{\mu}_5 \nu(n,\tilde{\mu}_6)}{K-k}\right.$$

$$\left. - \frac{\mu_3 \nu(n,\mu_4) - \tilde{\mu}_5 \nu(n,\tilde{\mu}_6)}{K-k-m}\right), \quad (A.15)$$

where $\mu_3 = e^{\frac{K-k-m(1+\varepsilon_0)(1+\varepsilon_s)}{P_s}}$ and $\mu_4 = \frac{K-k-m}{P_s \eta_0} - \frac{mP_0}{P_s}$. In step (b) of (A.15), we have replaced $\binom{K-k-2}{i}$ with $\binom{K-k-1}{i+1}\frac{i+1}{K-k-1}$, applied $m = i + 1$, and added term for $m = 0$ without changing the value of $P_{\text{out}}^{(\text{II},k)}$ since $\frac{\tilde{\mu}_1 \nu(n,\tilde{\mu}_2) - \tilde{\mu}_5 \nu(n,\tilde{\mu}_6)}{K-k} - \frac{\mu_3 \nu(n,\mu_4) - \tilde{\mu}_5 \nu(n,\tilde{\mu}_6)}{K-k-m} = 0$ when $m = 0$.

Furthermore, some terms in (A.15) involving $\tilde{\mu}_1$, $\tilde{\mu}_2$, $\tilde{\mu}_5$, and $\tilde{\mu}_6$ but being independent of m can be further eliminated since $\sum_{m=0}^{k} \binom{k}{m}(-1)^m = 0$, while $\tilde{\mu}_1$, $\tilde{\mu}_2$, $\tilde{\mu}_5$, and $\tilde{\mu}_6$ are not functions of m. The simplification can be expressed as follows:

$$P_{\text{out}}^{(\text{II},k)} = \frac{\tilde{\varphi}_k}{k(K-k-1)} \sum_{m=0}^{K-k-1} \binom{K-k-1}{m} (-1)^m$$

$$\times \sum_{n=0}^{k} \binom{k}{n} (-1)^n e^{\frac{n}{P_s}} \frac{\mu_3 \nu(n,\mu_4) - \tilde{\mu}_5 \nu(n,\tilde{\mu}_6)}{K-k-m}$$

$$\stackrel{(c)}{=} \varphi_k \sum_{m=0}^{K-k} \binom{K-k}{m} (-1)^m$$

$$\times \sum_{n=0}^{k} \binom{k}{n} (-1)^n e^{\frac{n}{P_s}} \left(\mu_3 \nu(n,\mu_4) - \tilde{\mu}_5 \nu(n,\tilde{\mu}_6)\right)$$

$$\stackrel{(d)}{=} \varphi_k \sum_{m=0}^{K-k} \binom{K-k}{m} (-1)^m$$

$$\times \sum_{n=0}^{k} \binom{k}{n} (-1)^n e^{\frac{n}{P_s}} \mu_3 \nu(n,\mu_4), \quad (A.16)$$

where step (c) follows by absorbing $K - k - 1$ into the binomial coefficients without changing the summation and step (d) follows by using $\sum_{m=0}^{k} \binom{k}{m}(-1)^m = 0$ and $\tilde{\mu}_5$ and $\tilde{\mu}_6$ that are not functions of m.

C. EVALUATION OF $P_{\text{OUT}}^{(\text{II},K-1)}$

The probability term $P_{\text{out}}^{(\text{II},K-1)}$ can be expressed as:

$$P_{\text{out}}^{(\text{II},K-1)} = \mathbb{E}_{|h_0|^2 > \eta_0} \left\{ \Pr\left(|h_{K-1}|^2 < \frac{P_0 \varepsilon_0^{-1}|h_0|^2 - 1}{P_s},\right.\right.$$

$$|h_K|^2 > \frac{P_0 \varepsilon_0^{-1}|h_0|^2 - 1}{P_s}, |h_K|^2$$

$$\left.\left. < \frac{(1+\varepsilon_s)(1+\varepsilon_0) - \left(1+P_0|h_0|^2\right)}{P_s}\right)\right\}.$$
(A.17)

By extracting the hidden constraint on the upper and lower bounds on $|h_K|^2$ from (A.17), i.e., $\frac{P_0 \varepsilon_0^{-1}|h_0|^2 - 1}{P_s} < \frac{(1+\varepsilon_s)(1+\varepsilon_0)-(1+P_0|h_0|^2)}{P_s}$, $P_{\text{out}}^{(\text{II},K-1)}$ can be rewritten as follows:

$$P_{\text{out}}^{(\text{II},K-1)} = \mathbb{E}_{\eta_0 < |h_0|^2 < (1+\varepsilon_s)\eta_0} \{S_{K-1}\}, \quad (A.18)$$

where S_{K-1} denotes probability inside the expectation in (A.17). There are two order statistics h_{K-1} and h_K involving in S_{K-1} with the joint PDF [44]

$$f_{|h_{K-1}|^2,|h_K|^2}(x,y) = \varphi_0 e^{-x}\left(1-e^{-x}\right)^{K-2} e^y, \quad (A.19)$$

where $x \le y$. Using (A.19), S_{K-1} can be evaluated as follows:

$$S_{K-1} = \varphi_0 \sum_{n=0}^{K-1} \binom{K-1}{n} \frac{(-1)^n e^{\frac{n}{P_s}} e^{-\frac{n|h_0|^2}{P_s \eta_0}}}{K-1}$$

$$\times \left(e^{\frac{1}{P_s}} e^{-\mu_5|h_0|^2} - e^{-\frac{\varepsilon_0+\varepsilon_s+\varepsilon_0\varepsilon_s}{P_s}} e^{-\mu_6|h_0|^2}\right), \quad (A.20)$$

where $\mu_5 = \frac{1}{P_s \eta_0}$ and $\mu_6 = -\frac{P_0}{P_s}$. Using the expression in (A.6), $P_{\text{out}}^{(\text{II},K-1)}$ can be derived as follows:

$$P_{\text{out}}^{(\text{II},K-1)} = \frac{\varphi_0}{K-1} \sum_{n=0}^{K-1} \binom{K-1}{n} (-1)^n e^{\frac{n}{P_s}}$$

$$\times \left(e^{\frac{1}{P_s}} \nu(n,\mu_5) - e^{-\frac{\varepsilon_0+\varepsilon_s+\varepsilon_0\varepsilon_s}{P_s}} \nu(n,\mu_6)\right). \quad (A.21)$$

D. EVALUATION OF $P_{OUT}^{(I)}$ AND $P_{OUT}^{(III)}$

In Case I, the determination of $P_{\text{out}}^{(I)}$ involves two independent random variables $|h_0|^2$ and $|h_K|^2$. Recalling the expression in (23), $P_{\text{out}}^{(I)}$ can be rewritten as follows:

$$P_{\text{out}}^{(I)} = \mathop{\mathbb{E}}_{|h_0|^2 > \eta_0} \left\{ \Pr\left(|h_K|^2 < \frac{\eta_0^{-1}|h_0|^2 - 1}{P_s}, |h_K|^2 < \frac{\varepsilon_s}{P_s} \right) \right\}. \tag{A.22}$$

By comparing $\frac{\eta_0^{-1}|h_0|^2 - 1}{P_s}$ and $\frac{\varepsilon_s}{P_s}$, it can be seen that $\frac{\eta_0^{-1}|h_0|^2 - 1}{P_s} < \frac{\varepsilon_s}{P_s}$ if $|h_0|^2 < \eta_0(1 + \varepsilon_s)$; Otherwise, $\frac{\eta_0^{-1}|h_0|^2 - 1}{P_s} > \frac{\varepsilon_s}{P_s}$. Thus, $P_{\text{out}}^{(I)}$ can be evaluated as follows:

$$
\begin{aligned}
P_{\text{out}}^{(I)} &= \mathop{\mathbb{E}}_{\eta_0 < |h_0|^2 < \eta_0(1+\varepsilon_s)} \left\{ \Pr\left(|h_K|^2 < \frac{\eta_0^{-1}|h_0|^2 - 1}{P_s} \right) \right\} \\
&\quad + \mathop{\mathbb{E}}_{|h_0|^2 > \eta_0(1+\varepsilon_s)} \left\{ \Pr\left(|h_K|^2 < \eta_s \right) \right\} \\
&= \int_{\eta_0}^{\eta_0(1+\varepsilon_s)} \left(1 - e^{-\frac{\eta_0^{-1}x - 1}{P_s}} \right)^K e^{-x} dx \\
&\quad + \left(1 - e^{-\eta_s} \right)^K e^{-\eta_0(1+\varepsilon_s)} \\
&= \sum_{n=0}^{K} \binom{K}{n} (-1)^n e^{\frac{n}{P_s}} \int_{\eta_0}^{\eta_0(1+\varepsilon_s)} e^{-\left(\frac{n}{P_s \eta_0} + 1 \right)x} dx \\
&\quad + \left(1 - e^{-\eta_s} \right)^K e^{-\eta_0(1+\varepsilon_s)} \\
&= \sum_{n=0}^{K} \binom{K}{n} (-1)^n e^{\frac{n}{P_s}} \nu(n, 0) \\
&\quad + \left(1 - e^{-\eta_s} \right)^K e^{-\eta_0(1+\varepsilon_s)}. \tag{A.23}
\end{aligned}
$$

Similarly to $P_{\text{out}}^{(I)}$, $P_{\text{out}}^{(III)}$ is a function of two independent random variables $|h_0|^2$ and $|h_K|^2$. In Case III, the achievable rate is $R_K^{(III)} = \log_2\left(1 + \frac{P_s|h_K|^2}{P_0|h_0|^2 + 1} \right)$ and $\tau = 0$. Then, $P_{\text{out}}^{(III)}$ can be evaluated as follows:

$$
\begin{aligned}
P_{\text{out}}^{(III)} &= \Pr\left(|h_0|^2 < \eta_0, \log_2\left(1 + \frac{P_s|h_K|^2}{P_0|h_0|^2 + 1} \right) < \hat{R}_s \right) \\
&= \sum_{n=0}^{K} \binom{K}{n} (-1)^n e^{-n\eta_s} \frac{1 - e^{-(1+n\eta_s P_0)\eta_0}}{1 + n\eta_s P_0}. \tag{A.24}
\end{aligned}
$$

By combing the obtained expressions for $P_{\text{out}}^{(I)}$, $P_{\text{out}}^{(II)}$, and $P_{\text{out}}^{(III)}$, we arrive at (28).

APPENDIX B
PROOF OF COROLLARY 1

Considering that $P_{\text{out}}^{(I)}$, $P_{\text{out}}^{(II)}$, and $P_{\text{out}}^{(III)}$ depend on k, the high SNR approximations for $P_{\text{out}}^{(I)}$, $P_{\text{out}}^{(II)}$, and $P_{\text{out}}^{(III)}$ will be derived separately in the following subsections.

A. HIGH SNR APPROXIMATION FOR $P_{OUT}^{(II,0)}$

Based on the derived closed-form expression in (A.9), $P_{\text{out}}^{(II,0)}$ can be rewritten as follows:

$$P_{\text{out}}^{(II,0)} = \frac{\varphi_0}{K(K-1)} \sum_{n=0}^{K} \binom{K}{n} (-1)^n \mu_1 \nu(0, \mu_2).$$

$$
\begin{aligned}
&= \frac{\varphi_0}{K(K-1)} \sum_{n=0}^{K} \binom{K}{n} (-1)^n \\
&\quad \times \mu_1 \int_{\eta_0}^{\eta_0(1+\varepsilon_s)} e^{-(\mu_2 + 1)x} dx. \tag{B.1}
\end{aligned}
$$

By applying the approximation $e^{-x} \approx 1 - x$ for $x \to 0$ and using the definitions of μ_1 and μ_2, as $P_0 = P_s \to \infty$, $P_{\text{out}}^{(II,0)}$ can be approximated as follows:

$$
\begin{aligned}
P_{\text{out}}^{(II,0)} &= \frac{\varphi_0}{K(K-1)} \int_{\eta_0}^{\eta_0(1+\varepsilon_s)} \sum_{n=0}^{K} \binom{K}{n} (-1)^n \\
&\quad \times e^{-\frac{n(1+\varepsilon_0)(1+\varepsilon_s)}{P_s}} e^{n\left(\varepsilon_0^{-1} + 1 \right)x} dx \\
&\overset{(e)}{=} \frac{\varphi_0}{K(K-1)} \\
&\quad \times \int_{\eta_0}^{\eta_0(1+\varepsilon_s)} \left(1 - e^{-\left(\frac{(1+\varepsilon_0)(1+\varepsilon_s)}{P_s} - \left(\varepsilon_0^{-1} + 1 \right)x \right)} \right)^K dx \\
&= \frac{\varphi_0}{K(K-1)} \\
&\quad \times \int_{\eta_0}^{\eta_0(1+\varepsilon_s)} \left(\frac{(1+\varepsilon_0)(1+\varepsilon_s)}{P_s} - \left(\varepsilon_0^{-1} + 1 \right)x \right)^K dx, \tag{B.2}
\end{aligned}
$$

where step (e) is obtained by applying $\sum_{n}^{K} \binom{K}{n} (-1)^n a^n = (1-a)^K$. By applying the binomial expansion, $P_{\text{out}}^{(II,0)}$ can be further simplified as follows:

$$
\begin{aligned}
P_{\text{out}}^{(II,0)} &= \frac{\varphi_0}{K(K-1)} \sum_{n=0}^{K} \binom{K}{n} \left(\frac{(1+\varepsilon_0)(1+\varepsilon_s)}{P_s} \right)^{K-n} \\
&\quad \times (-1)^n \left(\varepsilon_0^{-1} + 1 \right)^n \int_{\eta_0}^{\eta_0(1+\varepsilon_s)} x^n dx \\
&= \frac{\varphi_0 \varepsilon_0 (1+\varepsilon_0)^K}{P_s^{K+1} K(K-1)} \sum_{n=0}^{K} \binom{K}{n} \frac{(-1)^n}{n+1} \\
&\quad \times \left((1+\varepsilon_s)^{K+1} - (1+\varepsilon_s)^{K-n} \right). \tag{B.3}
\end{aligned}
$$

B. HIGH SNR APPROXIMATION FOR $P_{OUT}^{(II,K)}$ WITH $1 \leq K \leq K - 2$

Reflecting to the derivations made in Appendix A, $P_{\text{out}}^{(II,k)}$ can be rewritten as follows:

$$
\begin{aligned}
P_{\text{out}}^{(II,k)} &= \varphi_k \sum_{m=0}^{K-k} \binom{K-k}{m} (-1)^m \sum_{n=0}^{k} \binom{k}{n} (-1)^n e^{\frac{n}{P_s}} \mu_3 \\
&\quad \times \int_{\eta_0}^{\eta_0(1+\varepsilon_k)} e^{-\left(\frac{n}{P_s \eta_0} + \mu_4 + 1 \right)x} dx. \tag{B.4}
\end{aligned}
$$

By applying the approximation $e^{-x} \approx 1 - x$ for $x \to 0$ and using the definitions of μ_3 and μ_4, as $P_0 = P_s \to \infty$, $P_{\text{out}}^{(II,k)}$ can be approximated as follows:

$$
\begin{aligned}
P_{\text{out}}^{(II,k)} &= \varphi_k \sum_{m=0}^{K-k} \binom{K-k}{m} (-1)^m \\
&\quad \times \sum_{n=0}^{k} \binom{k}{n} (-1)^n e^{\frac{n}{P_s}} e^{-\frac{m(1+\varepsilon_0)(1+\varepsilon_s)}{P_s}}
\end{aligned}
$$

$$\times \int_{\eta_0}^{\eta_0(1+\varepsilon_k)} e^{-\left(\frac{n}{P_k\eta_0} - \frac{m}{P_s\eta_0} - m\right)x} dx. \quad (B.5)$$

Since $\sum_{n=0}^{k} \binom{k}{n}(-1)^n a^n = (1-a)^k$, $P_{\text{out}}^{(\text{II},k)}$ can be further expressed as follows:

$$
\begin{aligned}
P_{\text{out}}^{(\text{II},k)} &= \varphi_k \int_{\eta_0}^{\eta_0(1+\varepsilon_s)} \sum_{m=0}^{K-k}\binom{K-k}{m}(-1)^m \sum_{n=0}^{k}\binom{k}{n}(-1)^n \\
&\quad \times e^{-n\left(\frac{(1+\varepsilon_0)(1+\varepsilon_s)}{P_s} - \left(\varepsilon_0^{-1}+1\right)x\right)} e^{-n\left(\varepsilon_0^{-1}x - P_s^{-1}\right)} dx \\
&= \varphi_k \int_{\eta_0}^{\eta_0(1+\varepsilon_k)} \left(1 - e^{-\left(\frac{(1+\varepsilon_0)(1+\varepsilon_s)}{P_s} - \left(\varepsilon_0^{-1}+1\right)x\right)}\right)^{K-k} \\
&\quad \times \left(1 - e^{-\left(\varepsilon_0^{-1}x - P_s^{-1}\right)}\right)^{k} dx \\
&\stackrel{(f)}{=} \varphi_k \int_{\eta_0}^{\eta_0(1+\varepsilon_k)} \left(\frac{(1+\varepsilon_0)(1+\varepsilon_s)}{P_s} - \left(\varepsilon_0^{-1}+1\right)x\right)^{K-k} \\
&\quad \times \left(\varepsilon_0^{-1}x - P_s^{-1}\right)^{k} dx, \quad (B.6)
\end{aligned}
$$

where step (f) follows high SNR approximations. Applying the binomial expansions to (B.6), the high SNR approximation for $P_{\text{out}}^{(\text{II},k)}$ can be obtained as follows:

$$
\begin{aligned}
P_{\text{out}}^{(\text{II},k)} &= \frac{\varphi_k \varepsilon_0 (1+\varepsilon_0)^{K-k}(-1)^k}{P_s^{K+1}} \\
&\quad \times \sum_{m=0}^{K-k}\binom{K-k}{m}(-1)^m (1+\varepsilon_s)^{K-k-m} \\
&\quad \times \sum_{n=0}^{k}\binom{k}{n}(-1)^n \frac{(1+\varepsilon_s)^{m+n+1}-1}{m+n+1}. \quad (B.7)
\end{aligned}
$$

C. HIGH SNR APPROXIMATION FOR $P_{\text{OUT}}^{(\text{II},K-1)}$

First, we rewrite $P_{\text{out}}^{(\text{II},K-1)}$ as follows:

$$
\begin{aligned}
P_{\text{out}}^{(\text{II},K-1)} &= \frac{\varphi_0}{K-1} \sum_{n=0}^{K-1}\binom{K-1}{n}(-1)^n e^{\frac{n}{P_s}} \\
&\quad \times \left(e^{\frac{1}{P_s}} \nu(n, \mu_5) - e^{-\frac{\varepsilon_0+\varepsilon_s+\varepsilon_0\varepsilon_s}{P_s}} \nu(n, \mu_6)\right) \\
&= \frac{\varphi_0}{K-1} \sum_{n=0}^{K-1}\binom{K-1}{n}(-1)^n e^{\frac{n}{P_s}} \\
&\quad \times \int_{\eta_0}^{\eta_0(1+\varepsilon_k)} \left(e^{\frac{1}{P_s}} e^{-\left(\frac{n}{P_k\eta_0}+\mu_5+1\right)x}\right. \\
&\quad \left. - e^{-\frac{\varepsilon_0+\varepsilon_s+\varepsilon_0\varepsilon_s}{P_s}} e^{-\left(\frac{n}{P_k\eta_0}+\mu_6+1\right)x}\right) dx. \quad (B.8)
\end{aligned}
$$

Since $\sum_{n=0}^{k}\binom{k}{n}(-1)^n = 0$, $P_{\text{out}}^{(\text{II},K-1)}$ can be expressed as follows:

$$
\begin{aligned}
P_{\text{out}}^{(\text{II},K-1)} &= \frac{\varphi_0}{K-1} \int_{\eta_0}^{\eta_0(1+\varepsilon_s)} \left(e^{\frac{1}{P_s}-\left(\varepsilon_0^{-1}+1\right)x} - e^{-\frac{\varepsilon_0+\varepsilon_s+\varepsilon_0\varepsilon_s}{P_s}}\right) \\
&\quad \times \left(1 - e^{-n\left(\varepsilon_0^{-1}x - P_s^{-1}\right)}\right)^{K-1} dx. \quad (B.9)
\end{aligned}
$$

By applying the approximations $e^{-x} \approx 1-x$ for $x \to 0$, as $P_0 = P_s \to \infty$, $P_{\text{out}}^{(\text{II},K-1)}$ can be approximated as follows:

$$
\begin{aligned}
P_{\text{out}}^{(\text{II},K-1)} &= \frac{\varphi_0}{K-1} \int_{\eta_0}^{\eta_0(1+\varepsilon_s)} \left(\varepsilon_0^{-1}x - P_s^{-1}\right)^{K-1} \\
&\quad \times \left(\frac{(1+\varepsilon_0)(1+\varepsilon_s)}{P_s} - \left(\varepsilon_0^{-1}+1\right)x\right) dx \\
&= \frac{\varphi_0}{K-1} \int_{\eta_0}^{\eta_0(1+\varepsilon_s)} \varepsilon_0^{-(K-1)}\left(x - \frac{\varepsilon_0}{P_s}\right)^{K-1} \\
&\quad \times \left(\frac{(1+\varepsilon_0)(1+\varepsilon_s)}{P_s} - \left(\varepsilon_0^{-1}+1\right)x\right) dx \\
&= \frac{\varphi_0}{K-1} \int_{\eta_0}^{\eta_0(1+\varepsilon_s)} \varepsilon_0^{-(K-1)} \frac{(1+\varepsilon_0)(1+\varepsilon_s)}{P_s} \\
&\quad \times \left(x - \frac{\varepsilon_0}{P_s}\right)^{K-1} dx \\
&\quad - \frac{\varphi_0}{K-1} \int_{\eta_0}^{\eta_0(1+\varepsilon_s)} \varepsilon_0^{-(K-1)}\left(\varepsilon_0^{-1}+1\right)x \\
&\quad \times \left(x - \frac{\varepsilon_0}{P_s}\right)^{K-1} dx \\
&= \frac{\varphi_0 \varepsilon_0 \varepsilon_s^K (1+\varepsilon_0)(1+\varepsilon_s)}{P_s^{K+1}K(K-1)} \\
&\quad - \frac{\varphi_0 \varepsilon_s^K\left(\varepsilon_0^{-1}+1\right)(K(1+\varepsilon_s)+1)}{P_s^{K+1}K(K-1)(K+1)}. \quad (B.10)
\end{aligned}
$$

Following similar algebraic manipulations as for deriving the high SNR approximation of $P_{\text{out}}^{(\text{II},k)}$ ($1 \le k \le K-1$), $P_{\text{out}}^{(\text{I})}$ and $P_{\text{out}}^{(\text{III})}$ can be approximated as

$$P_{\text{out}}^{(\text{I})} = \frac{\varepsilon_0 \varepsilon_s^{K+1}}{P_s^{K+1}(K+1)} + \frac{\varepsilon_s^K}{P_s^K} - \frac{\varepsilon_0 \varepsilon_s^K(1+\varepsilon_s)}{P_s^{K+1}} \quad (B.11)$$

and

$$
\begin{aligned}
P_{\text{out}}^{(\text{III})} &= \frac{\varepsilon_s^K\left((1+\varepsilon_0)^{K+1}-1\right)}{P_s^{K+1}(K+1)} \\
&\quad - \frac{\varepsilon_s^K\left((\varepsilon_0(K+1)-1)(1+\varepsilon_0)^{K+1}+1\right)}{P_s^{K+2}(K+2)(K+1)}, \quad (B.12)
\end{aligned}
$$

respectively.

By combing (B.3), (B.7), (B.10), (B.11), and (B.12), the high SNR approximation for P_{out} is obtained as (33).

REFERENCES

[1] Z. Zhang et al., "6G wireless networks: Vision, requirements, architecture, and key technologies," *IEEE Veh. Technol. Mag.*, vol. 14, no. 3, pp. 28–41, Sep. 2019.

[2] "Roadmap for IoT research, innovation and development in europe," EU NGIoT, Novi Sad, Serbia, Jan. 2020.

[3] L. Liu, E. G. Larsson, W. Yu, P. Popovski, C. Stefanovic, and E. de Carvalho, "Sparse signal processing for grant-free massive connectivity: A future paradigm for random access protocols in the Internet of Things," *IEEE Signal Process. Mag.*, vol. 35, no. 5, pp. 88–99, Sep. 2018.

[4] A. Bayesteh, E. Yi, H. Nikopour, and H. Baligh, "Blind detection of SCMA for uplink grant-free multiple-access," in *Proc. Int. Symp. Wireless Commun. Syst. (ISWCS)*, Barcelona, Spain, Aug. 2014, pp. 1–6.

[5] Z. Ding, R. Schober, P. Fan, and H. V. Poor, "Simple semi-grant-free transmission strategies assisted by non-orthogonal multiple access," *IEEE Trans. Commun.*, vol. 67, no. 6, pp. 4464–4478, Jun. 2019.

[6] Z. Ding, R. Schober, and H. V. Poor, "A new QoS-guarantee strategy for NOMA assisted semi-grant-free transmission," *IEEE Trans. Commun.*, vol. 69, no. 11, pp. 7489–7503, Nov. 2021.

[7] C. Zhang, Z. Qin, Y. Liu, and K. K. Chai, "Semi-grant-free uplink NOMA with contention control: A stochastic geometry model," in *Proc. IEEE Int. Conf. Commun. Workshops*, Dubin, Ireland, Jun. 2020, pp. 1–6.

[8] H. Lu, X. Xie, Z. Shi, H. Lei, H. Yang, and J. Cai, "Advanced NOMA assisted semi-grant-free transmission schemes for randomly distributed users." 2020. [Online]. Available: https://arxiv.org/abs/2012.09423.

[9] Z. Ding, R. Schober, and H. V. Poor, "Unveiling the importance of SIC in NOMA systems—Part I: State of the art and recent findings," *IEEE Commun. Lett.*, vol. 24, no. 11, pp. 2373–2377, Nov. 2020.

[10] Z. Yang, P. Xu, J. Ahmed Hussein, Y. Wu, Z. Ding, and P. Fan, "Adaptive power allocation for uplink non-orthogonal multiple access with semi-grant-free transmission," *IEEE Wireless Commun. Lett.*, vol. 9, no. 10, pp. 1725–1729, Oct. 2020.

[11] Z. Ding, P. Fan, and H. V. Poor, "Impact of user pairing on 5G nonorthogonal multiple-access downlink transmissions," *IEEE Trans. Veh. Technol.*, vol. 65, no. 8, pp. 6010–6023, Aug. 2016.

[12] H. Liu, T. A. Tsiftsis, K. J. Kim, K. S. Kwak, and H. V. Poor, "Rate splitting for uplink NOMA with enhanced fairness and outage performance," *IEEE Trans. Wireless Commun.*, vol. 19, no. 7, pp. 4657–4670, Jul. 2020.

[13] Y. Sun, Z. Ding, and X. Dai, "A new design of hybrid SIC for improving transmission robustness in uplink NOMA," *IEEE Trans. Veh. Technol.*, vol. 70, no. 5, pp. 5083–5087, May 2021.

[14] B. Rimoldi and R. Urbanke, "A rate-splitting approach to the Gaussian multiple-access channel," *IEEE Trans. Inf. Theory*, vol. 42, no. 2, pp. 364–375, Mar. 1996.

[15] H. Liu, Z. Bai, H. Lei, G. Pan, K. J. Kim, and T. A. Tsiftsis, "A new rate splitting strategy for uplink CR-NOMA systems," *IEEE Trans. Veh. Technol.*, vol. 71, no. 7, pp. 7947–7951, Jul. 2022.

[16] Y. Mao, O. Dizdar, B. Clerckx, R. Schober, P. Popovski, and H. V. Poor, "Rate-splitting multiple access: Fundamentals, survey, and future research trends," *IEEE Commun. Surveys Tuts.*, vol. 24, no. 4, pp. 2073–2126, 4th Quart., 2022.

[17] A. Mishra, Y. Mao, O. Dizdar, and B. Clerckx, "Rate-splitting multiple access for 6G–Part I: Principles, applications and future works." 2022. [Online]. Available: https://arxiv.org/abs/2205.02548.

[18] B. Clerckx, H. Joudeh, C. Hao, M. Dai, and B. Rassouli, "Rate splitting for MIMO wireless networks: A promising PHY-layer strategy for LTE evolution," *IEEE Commun. Mag.*, vol. 54, no. 5, pp. 98–105, May 2016.

[19] Y. Mao, B. Clerckx, and V. O. K. Li, "Rate-splitting multiple access for downlink communication systems: Bridging, generalizing and outperforming SDMA and NOMA," *EURASIP J. Wireless Commun. Netw.*, vol. 2018, no. 1, pp. 1–54, May 2018.

[20] H. Joudeh and B. Clerckx, "Sum-rate maximization for linearly Precoded Downlink multiuser MISO systems with partial CSIT: A rate-splitting approach," *IEEE Trans. Commun.*, vol. 64, no. 11, pp. 4847–4861, Nov. 2016.

[21] B. Clerckx, Y. Mao, R. Schober, and H. V. Poor, "Rate-splitting unifying SDMA, OMA, NOMA, and multicasting in MISO broadcast channel: A simple two-user rate analysis," *IEEE Wireless Commun. Lett.*, vol. 9, no. 3, pp. 349–353, Mar. 2020.

[22] O. Dizdar, Y. Mao, W. Han, and B. Clerckx, "Rate-splitting multiple access: A new frontier for the PHY layer of 6G," in *Proc. IEEE 92nd Veh. Technol. Conf. (VTC-Fall)*, Victoria, BC, Canada, Dec. 2020, pp. 1–7.

[23] Z. Yang, M. Chen, W. Saad, W. Xu, and M. Shikh-Bahaei, "Sum-rate maximization of uplink rate splitting multiple access (RSMA) communication," *IEEE Trans. Mobile Comput.*, vol. 21, no. 7, pp. 2596–2609, Jul. 2022.

[24] J. Zeng, T. Lv, W. Ni, R. Liu, N. C. Beaulieu, and Y. J. Guo, "Ensuring max-min fairness of UL SIMO-NOMA: A rate splitting approach," *IEEE Trans. Veh. Technol.*, vol. 68, no. 11, pp. 11080–11093, Nov. 2019.

[25] Y. Zhu, Z. Zhang, X. Wang, and X. Liang, "A low-complexity non-orthogonal multiple access system based on rate splitting," in *Proc. 9th Int. Conf. Wireless Commun. Signal Process. (WCSP)*, Nanjing, China, Oct. 2017, pp. 1–6.

[26] Y. Zhu, X. Wang, Z. Zhang, X. Chen, and Y. Chen, "A rate-splitting non-orthogonal multiple access scheme for uplink transmission," in *Proc. 9th Int. Conf. Wireless Commun. Signal Process. (WCSP)*, Nanjing, China, Oct. 2017, pp. 1–6.

[27] E. J. D. Santos, R. D. Souza, and J. L. Rebelatto, "Rate-splitting multiple access for URLLC uplink in physical layer network slicing with eMBB," *IEEE Access*, vol. 9, pp. 163178–163187, 2021.

[28] O. Dizdar, Y. Mao, Y. Xu, P. Zhu, and B. Clerckx, "Rate-splitting multiple access for enhanced URLLC and eMBB in 6G," in *Proc. 17th Int. Symp. Wireless Commun. Syst. (ISWCS)*, Berlin, Germany, Sep. 2021, pp. 1–6.

[29] S. A. Tegos, P. D. Diamantoulakis, and G. K. Karagiannidis, "On the performance of uplink rate-splitting multiple access," *IEEE Commun. Lett.*, vol. 26, no. 3, pp. 523–527, Mar. 2022.

[30] O. Abbasi and H. Yanikomeroglu, "Rate-splitting and NOMA-enabled uplink user cooperation," in *Proc. IEEE Wireless Commun. Netw. Conf. Workshops (WCNCW)*, Nanjing, China, Mar. 2021, pp. 1–6.

[31] W. Jaafar, S. Naser, S. Muhaidat, P. C. Sofotasios, and H. Yanikomeroglu, "Multiple access in aerial networks: From orthogonal and non-orthogonal to rate-splitting," *IEEE Open J. Veh. Technol.*, vol. 1, pp. 372–392, Oct. 2020.

[32] H. Kong, M. Lin, Z. Wang, J.-Y. Wang, W.-P. Zhu, and J. Wang, "Performance analysis for rate splitting uplink NOMA transmission in high throughput satellite systems," *IEEE Wireless Commun. Lett.*, vol. 11, no. 4, pp. 816–820, Apr. 2022.

[33] A. Mishra, Y. Mao, L. Sanguinetti, and B. Clerckx, "Rate-splitting assisted massive machine-type communications in cell-free massive MIMO," *IEEE Commun. Lett.*, vol. 26, no. 6, pp. 1358–1362, Jun. 2022.

[34] M. Z. Hassan, M. J. Hossain, J. Cheng, and V. C. M. Leung, "Device-clustering and rate-splitting enabled device-to-device cooperation framework in fog radio access network," *IEEE Trans. Green Commun. Netw.*, vol. 5, no. 3, pp. 1482–1501, Sep. 2021.

[35] C. Zhang, Y. Liu, W. Yi, Z. Qin, and Z. Ding, "Semi-grant-free NOMA: Ergodic rates analysis with random deployed users," *IEEE Wireless Commun. Lett.*, vol. 10, no. 4, pp. 692–695, Apr. 2021.

[36] N. Jayanth, P. Chakraborty, M. Gupta, and S. Prakriya, "Performance of semi-grant free uplink with non-orthogonal multiple access," in *Proc. IEEE Int. Symp. Pers. Indoor Mobile Radio Commun.*, London, U.K., 2020, pp. 1–6.

[37] J. Ding, M. Feng, M. Nemati, and J. Choi, "Performance analysis of massive MIMO assisted semi-grant-free random access," in *Proc. IEEE 18th Annu. Consum. Commun. Netw. Conf. (CCNC)*, Las Vegas, NV, USA, Jan. 2021, pp. 1–7.

[38] D. Pliatsios, A.-A. A. Boulogeorgos, T. Lagkas, V. Argyriou, I. D. Moscholios, and P. G. Sarigiannidis, "Semi-grant-free non-orthogonal multiple access for tactile Internet of Things," in *Proc. IEEE Int. Symp. Pers. Indoor Mob. Radio Commun.*, Helsinki, Finland, 2021, pp. 1389–1394.

[39] W. Yi, W. Yu, Y. Liu, C. H. Foh, Z. Ding, and A. Nallanathan, "Multiple transmit power levels based NOMA for massive machine-type communications." 2020. [Online]. Available: https://arxiv.org/abs/2011.12388.

[40] M. Fayaz, W. Yi, Y. Liu, and A. Nallanathan. "Competitive MA-DRL for transmit power pool design in semi-grant-free NOMA systems." 2021. [Online]. Available: https://arxiv.org/abs/2106.11190.

[41] M. Fayaz, W. Yi, Y. Liu, and A. Nallanathan, "Transmit power pool design for grant-free NOMA-IoT networks via deep reinforcement learning," *IEEE Trans. Wireless Commun.*, vol. 20, no. 11, pp. 7626–7641, Nov. 2021.

[42] J. Chen, L. Guo, J. Jia, J. Shang, and X. Wang, "Resource allocation for IRS assisted SGF NOMA transmission: A MADRL approach," *IEEE J. Sel. Areas Commun.*, vol. 40, no. 4, pp. 1302–1316, Apr. 2022.

[43] H. Liu, Y. Ye, Z. Bai, K. J. Kim, and T. A. Tsiftsis, "Rate splitting multiple access aided mobile edge computing in cognitive radio networks," in *Proc. IEEE Int. Conf. Commun. Workshops (ICC Workshops)*, Seoul, South Korea, May 2022, pp. 598–603.

[44] H. A. David and H. N. Nagaraja, *Order Statistics*, 3rd ed. Hoboken, NJ, USA: Wiley, 2005.

FENGCHENG XIAO received the B.S. degree in electronic information engineering from Shandong Management University, Jinan, China, in 2021. He is currently pursuing the M.E. degree with the School of Information Science and Electrical Engineering, Shandong Jiaotong University, Jinan. His research interests include nonorthogonal multiple access, cognitive radios, and wireless secrecy communications.

XINGWANG LI (Senior Member, IEEE) received the M.Sc. degree from the University of Electronic Science and Technology of China, Chengdu, China, in 2010, and the Ph.D. degree from the Beijing University of Posts and Telecommunications, Beijing, China, in 2015.

From 2010 to 2012, he worked with Comba Telecom Ltd., Guangzhou, China, as an Engineer. He spent one year from 2017 to 2018, as a Visiting Scholar with Queen's University Belfast, Belfast, U.K. He is currently an Associated Professor with the School of Physics and Electronic Information Engineering, Henan Polytechnic University, Jiaozuo, China. His research interests include wireless communication, intelligent transport system, artificial intelligence, and Internet of Things. He serves as an Editor on the Editorial Board of IEEE TRANSACTIONS ON INTELLIGENT TRANSPORTATION SYSTEMS, IEEE TRANSACTIONS ON VEHICULAR TECHNOLOGY, IEEE SYSTEMS JOURNAL, IEEE SENSORS JOURNAL, and *Physical Communication*. He was also the Lead/Guest Editor for the special issue on Computational Intelligence and Advanced Learning for Next-Generation Industrial IoT of IEEE TRANSACTIONS ON NETWORK SCIENCE AND ENGINEERING, AI driven Internet of Medical Things for Smart Healthcare Applications: Challenges, and Future Trends in IEEE JOURNAL OF BIOMEDICAL AND HEALTH INFORMATICS, UAV-Enabled B5G/6G Networks: Emerging Trends and Challenges published in *Physical Communication*. He has served as a TPC member for many conferences, such as IEEE Globecom, IEEE WCNC, IEEE VTC, and IEEE ICCC. He has also served as the Co-Chair for IEEE/IET CSNDSP 2020 and 2022.

LIANG YANG (Senior Member, IEEE) was born in Hunan, China. He received the Ph.D. degree in electrical engineering from Sun Yat-sen University, Guangzhou, China, in 2006. From 2006 to 2013, he was a Faculty Member with Jinan University, Guangzhou. He joined the Guangdong University of Technology in 2013. He is currently a Professor with Hunan University, Changsha, China. His current research interests include the performance analysis of wireless communications systems.

HONGWU LIU (Senior Member, IEEE) received the Ph.D. degree from Southwest Jiaotong University in 2008. From 2008 to 2010, he was a Faculty Member with Nanchang Hangkong University. From 2010 to 2011, he was a Postdoctoral Fellow with the Shanghai Institute of Microsystem and Information Technology, Chinese Academy of Science. From 2011 to 2013, he was a Research Fellow with the UWB Wireless Communications Research Center, Inha University, South Korea. Since 2014, he has been an Associate Professor with Shandong Jiaotong University. His research interests include MIMO signal processing, cognitive radios, cooperative communications, and AI-based wireless communications.

THEODOROS A. TSIFTSIS (Senior Member, IEEE) received the Ph.D. degree in electrical engineering from the University of Patras, Greece, in 2006.

He is a Professor with the School of Intelligent Systems Science and Engineering, Jinan University, China, and also with the Department of Informatics and Telecommunications, University of Thessaly, Greece. His research interests fall into the broad areas of communication theory and wireless communications with emphasis on wireless communications theory, reconfigurable intelligent surfaces, optical wireless communications, and physical layer security. He served in the editorial boards for the IEEE TRANSACTIONS ON COMMUNICATIONS, IEEE TRANSACTIONS ON VEHICULAR TECHNOLOGY, and IEEE COMMUNICATIONS LETTERS. He is currently an Associate Editor of the IEEE TRANSACTIONS ON WIRELESS COMMUNICATIONS and IEEE TRANSACTIONS ON MOBILE COMPUTING. He was appointed as an IEEE Vehicular Technology Society Distinguished Lecturer for two terms from 2018 to 2022.